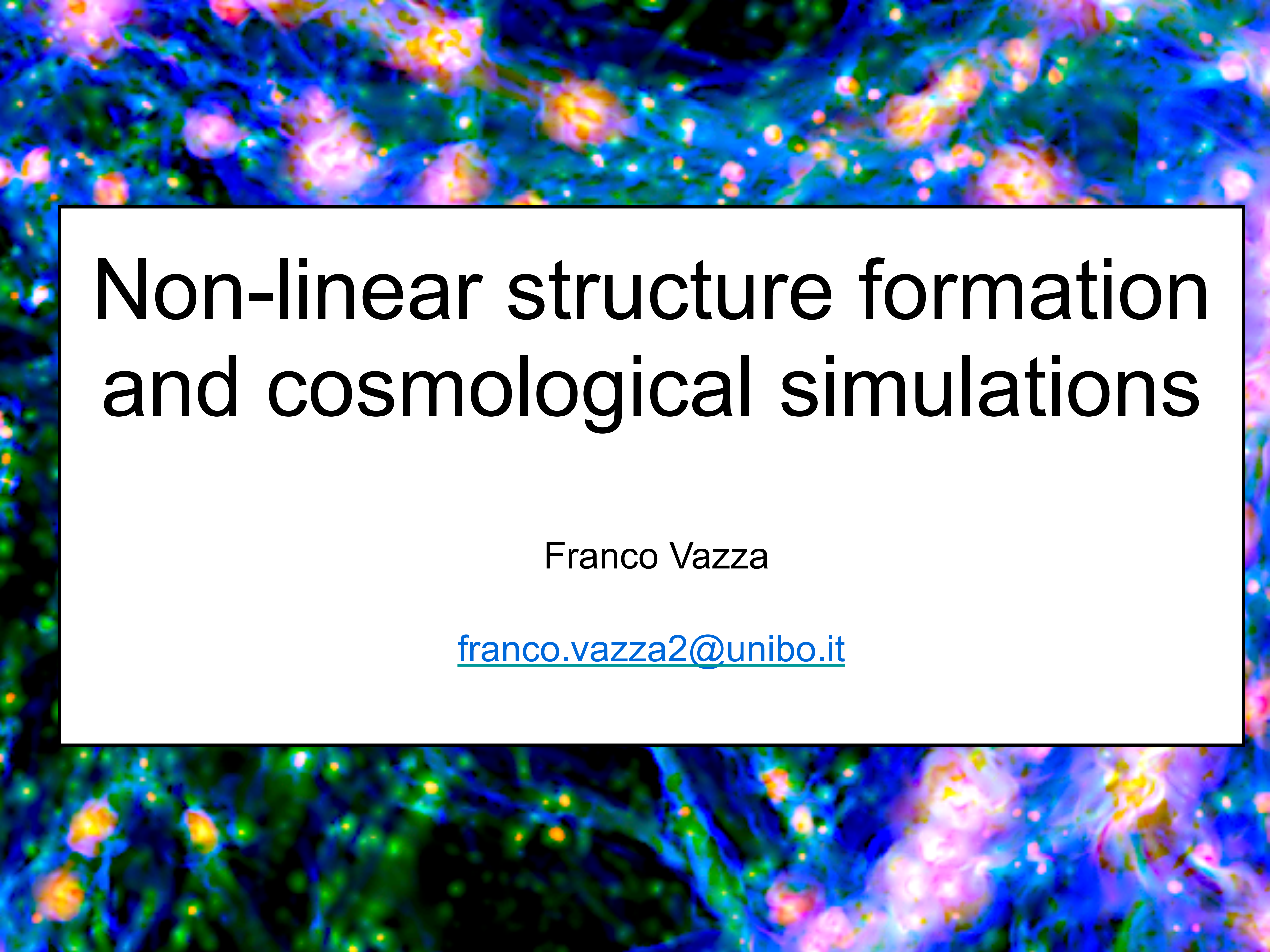

Non-linear structure formation and cosmological simulations

Franco Vazza

franco.vazza2@unibo.it

OUTLINE

In this lesson we will (briefly) see:

- how to describe the formation of the cosmic web
- what are the techniques for cosmological simulations
- what are the numerical problems and how to incorporate several physical mechanisms (including magnetic fields)

NON-LINEAR STRUCTURE FORMATION

Some important criticalities:

- gravity leads to high density contrasts: $\delta\rho/\rho \gg 1000$
- extremely wide range of spatial scales in processes (from ~kpc to ~100 Mpc), of density range ($\rho \sim 0.1 \langle\rho\rangle$ to $\rho \sim 10^4 \langle\rho\rangle$).
- supersonic converging flows (shocks) & sub-sonic turbulent flows (halos)
- galaxy formation physics can feedback on structure formation itself
- some phenomena "emerge" only at large enough dynamical range (e.g. turbulence, dynamo) $\rightarrow$ need of extremely large Reynolds number

numerical simulations needed

STRUCTURE FORMATION: THE ZELDOVICH APPROXIMATION

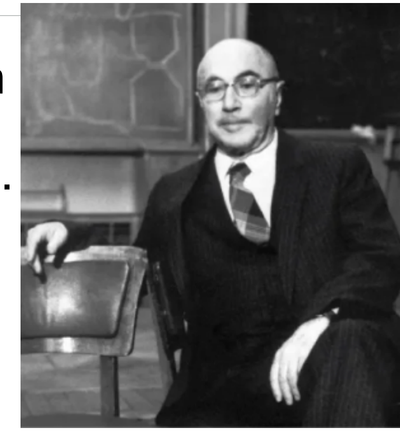

The "Zeldovich approximation" follows the motion of a fluid element in a Lagrangian-to-Eulerian mapping of the equations of hydrodynamics.

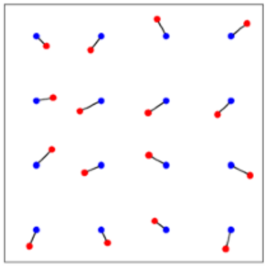

$$\mathbf{x}(\mathbf{q}, t) = \mathbf{q} + \Psi(\mathbf{q}, t)$$

where $\mathbf{q}$ is the initial position and $\Psi(\mathbf{q}, t)$ is the linear displacement field, given by

$$\Psi(\mathbf{q}, t) = D(t)\, \Psi_0(\mathbf{q})$$

where $D(t)$ is the linear growth factor seen yesterday and $\Psi_0(\mathbf{q}) = -\nabla \phi_0(\mathbf{q})$ is related to the initial density contrast via the Poisson equation: $\nabla^2 \phi_0 = \delta$

Mass conservation allows to relate the Eulerian overdensity field $\delta(\vec{x}, t)$ to the divergence of the displacement field:

$$\delta(\mathbf{q}, t) \simeq -D(t)\, \nabla \cdot \Psi_0(\mathbf{q})$$

STRUCTURE FORMATION: THE ZELDOVICH APPROXIMATION

To generate **initial conditions**, one has to generate a set of complex numbers with a randomly distributed phase ϕ and with amplitude normally distributed with a variance given by the desired power spectrum, P(k). This can be obtained by drawing two random numbers ϕ in]0, 1] and A in]0, 1] for every point in k-space.

$$\hat{\delta}_{\mathbf{k}} = \sqrt{-2P(|\mathbf{k}|)\ln(A)}\mathrm{e}^{i2\pi\phi}$$

To obtain the perturbation field generated from this distribution, one needs to generate the potential Φ(q) on a grid q in real space via a Fourier transform, e.g.

$$\Phi(\mathbf{q}) = \sum_k \frac{\hat{\delta}_{\mathbf{k}}}{\mathbf{k}^2}\mathrm{e}^{i\mathbf{kq}}$$

Then through the Zeldovich approximation we can update positions and velocities:

$$\mathbf{x} = \mathbf{q} - D^+(z)\Phi(\mathbf{q}) \qquad \mathbf{v} = \dot{D}^+(z)\nabla\Phi(\mathbf{q})$$

This powerful approach ceases its validity after the interpenetration of particle flows as it cannot capture the clustering due to self-gravity, as well as collisional effects in ordinary matter

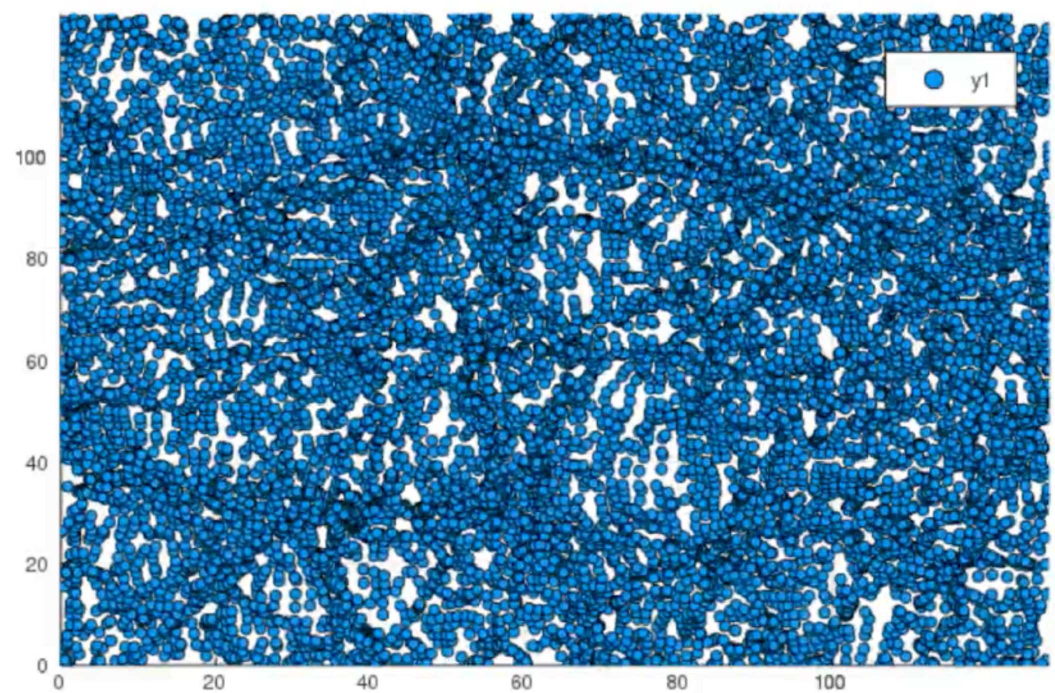

small (2D) N-boyd sim

STRUCTURE FORMATION: THE ZELDOVICH APPROXIMATION

To generate **initial conditions**, one has to generate a set of complex numbers with a randomly distributed phase ϕ and with amplitude normally distributed with a variance given by the desired power spectrum, P(k). This can be obtained by drawing two random numbers ϕ in]0, 1] and A in]0, 1] for every point in k-space.

$$\hat{\delta}_{\mathbf{k}} = \sqrt{-2P(|\mathbf{k}|)\ln(A)}\mathrm{e}^{i2\pi\phi}$$

To obtain the perturbation field generated from this distribution, one needs to generate the potential Φ(q) on a grid q in real space via a Fourier transform, e.g.

$$\Phi(\mathbf{q}) = \sum_k \frac{\hat{\delta}_{\mathbf{k}}}{\mathbf{k}^2}\mathrm{e}^{i\mathbf{kq}}$$

Then through the Zeldovich approximation we can update positions and velocities:

$$\mathbf{x} = \mathbf{q} - D^+(z)\Phi(\mathbf{q}) \qquad \mathbf{v} = \dot{D}^+(z)\nabla\Phi(\mathbf{q})$$

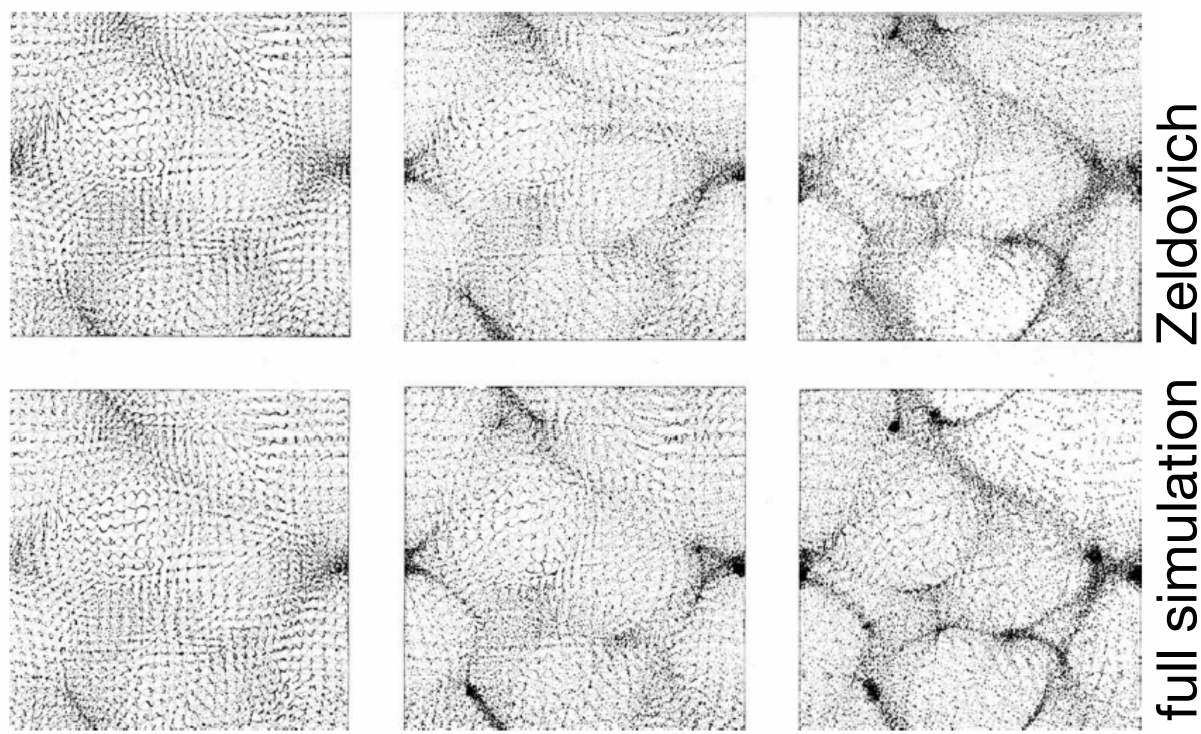

This powerful approach ceases its validity after the interpenetration of particle flows as it cannot capture the clustering due to self-gravity, as well as collisional effects in ordinary matter

STRUCTURE FORMATION: THE ZELDOVICH APPROXIMATION

Side note:
this process is a simple analogy with the formation of optical caustics at the bottom of a pool of water.
A uniform screen of light (top) first passes through tiny corrugations at the top of water.
While propagating to the bottom light rays start crossing each other and produce caustics of light, which resemble the formation of cosmological filaments (in this case, the vertical direction will be time dimension in cosmology)

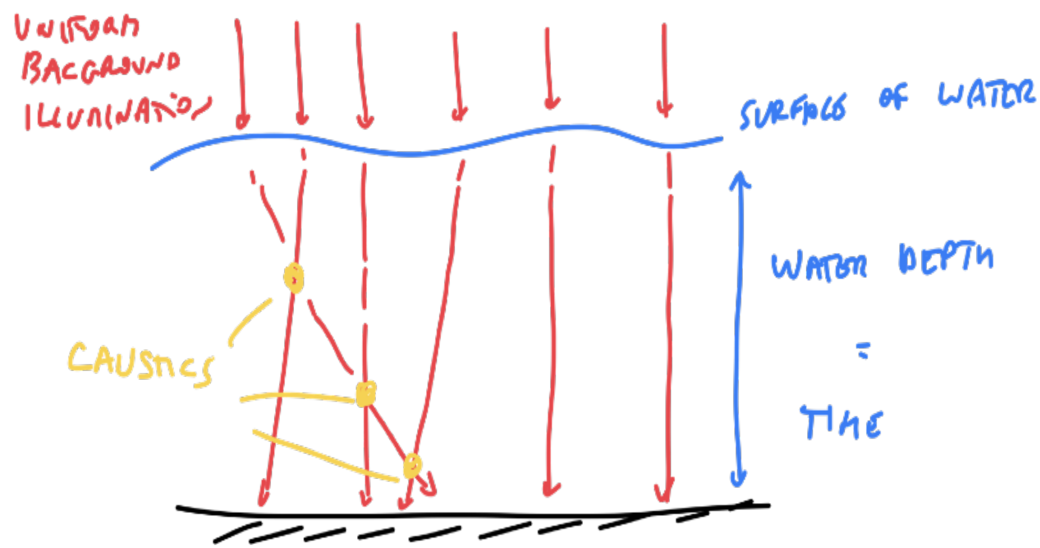

STRUCTURE FORMATION: THE ZELDOVICH APPROXIMATION

Side note:
this process is a simple analogy with the formation of optical caustics at the bottom of a pool of water.
A uniform screen of light (top) first passes through tiny corrugations at the top of water.
While propagating to the bottom light rays start crossing each other and produce caustics of light, which resemble the formation of cosmological filaments (in this case, the vertical direction will be time dimension in cosmology)

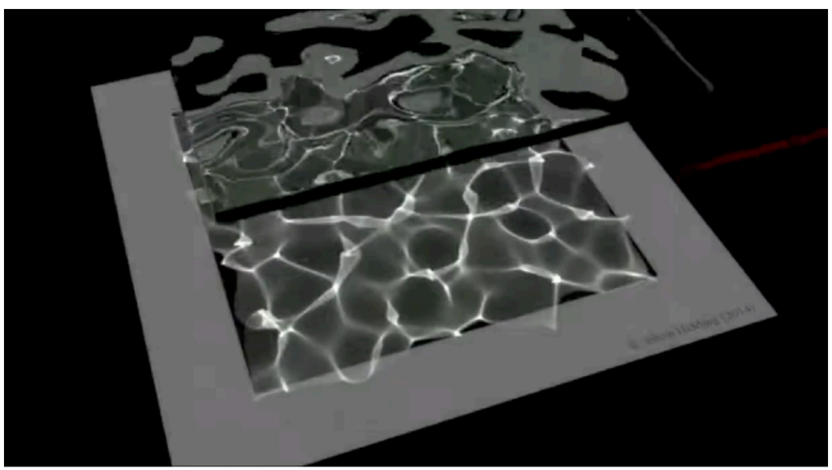

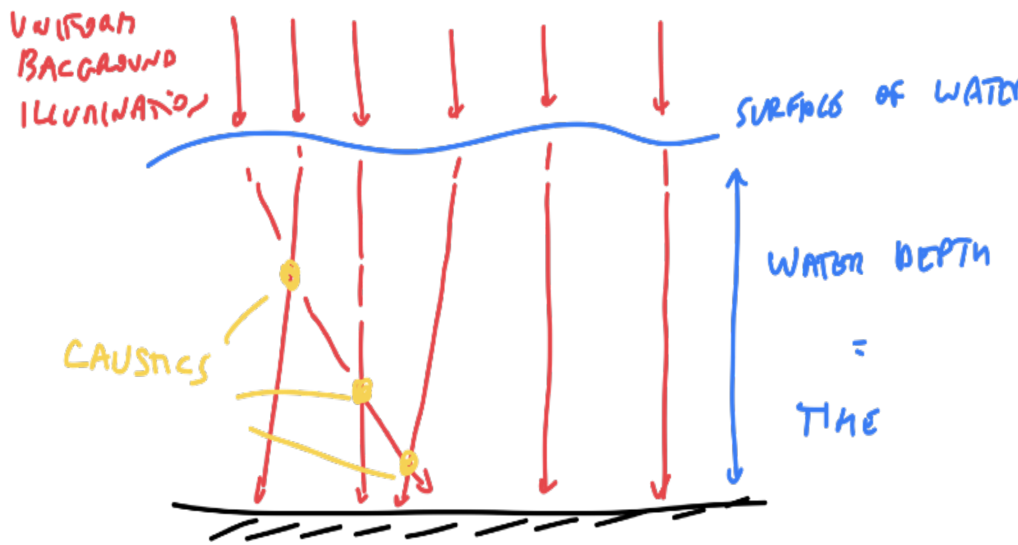

https://www.youtube.com/watch?v=0fjk8X1KuyE&t=1s

STRUCTURE FORMATION: THE ZELDOVICH PANCAKE

Basic steps described by the "Zeldovich pancake" model (1970) for the 1D collapse of cold, self-gravitating gas after a small velocity perturbation (even without dark matter)

1. a small $\delta\rho/\langle\rho\rangle \ll 1$ overdensity is formed
2. matter keeps falling towards the overdensity
3. when the infall velocity $v_{ff} \sim \sqrt{2GM/r}$ exceeds the sound speed, shocks are formed.
4. Kinetic infall energy is converted into thermal energy
5. An ~isothermal dense gas core $\delta\rho/\langle\rho\rangle \geq 10^2$with a declining density profile is formed.
6. Sharp boundaries with the outer (cold) Universe are marked by **strong accretion shocks** ($\mathscr{M} = v_{ff}/c_s \geq 10^2$)
7. the collapse is most probable to happen along 1 direction first, leading to a flat pancake structure

(The presence of dark matter alters the above picture by giving even more infall kinetic energy to the gas.)

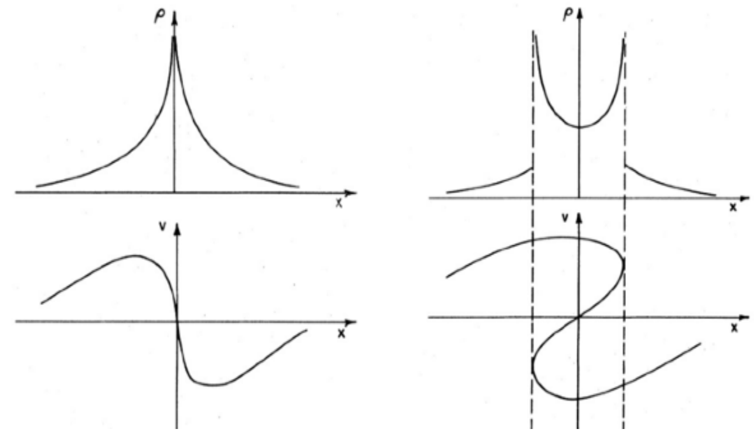

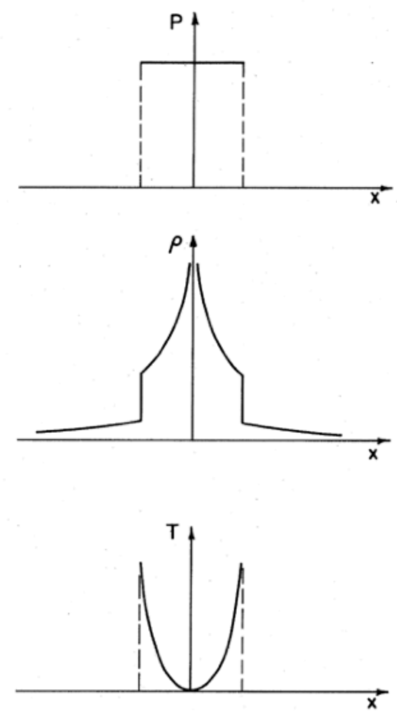

FIG. 6. Distributions of pressure (p), density (ρ), and temperature (T) a short time after the formation of a gas pancake.

STRUCTURE FORMATION: THE ZELDOVICH APPROXIMATION

The simulated 1D evolution of the Zeldovich pancake

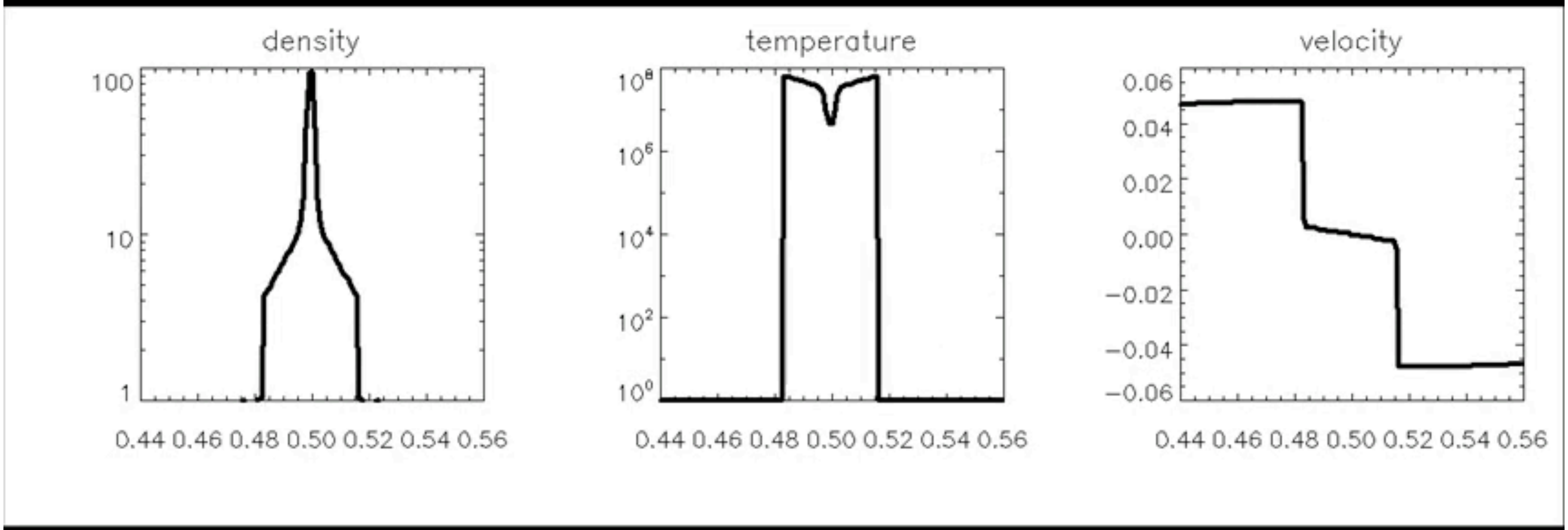

STRUCTURE FORMATION: THE ZELDOVICH APPROXIMATION

The linear theory of perturbations, applied to the uniform isotropic cosmological solution, is now well understood. It is generally admitted that its predictions are limited by $\delta\varrho/\varrho < 1$, and that further events must be followed by numerical calculations. Such calculations, in three dimensions and with random initial conditions, promise to be tedious. Therefore an approximate method, which gives the right answer at least qualitatively, is of interest.

SIMULATING COSMIC STRUCTURES

About 83% of matter is **Dark Matter**, so this is the first component to model. This is obtained by evolving a discrete distribution of point masses, and using trajectory integrator coupled to several possible gravity solvers

- force equation $$\frac{d\mathbf{p}}{dt} = -m\nabla\Phi$$ grav.potential

- velocity equation $$\frac{d\mathbf{x}}{dt} = \frac{\mathbf{p}}{ma^2}.$$ expansion terms

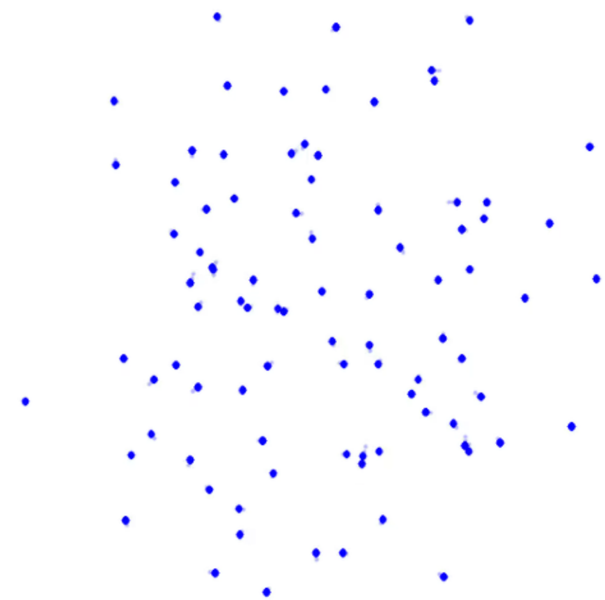

introducing the pecular velocity $\mathbf{v} = a\dot{\mathbf{x}}$

we can write: $$\frac{d\mathbf{v}}{dt} + \mathbf{v}\frac{\dot{a}}{a} = -\frac{\nabla\Phi}{a}.$$

- expansion rate $$\dot{a} = H_0\sqrt{1 + \Omega_0(a^{-1} - 1) + \Omega_\Lambda(a^2 - 1)},$$

Since Dark Matter is collision-less, it must be modelled

SIMULATING COSMIC STRUCTURES

Early “N-Body” simulation of a collision between galaxies

SIMULATING COSMIC STRUCTURES

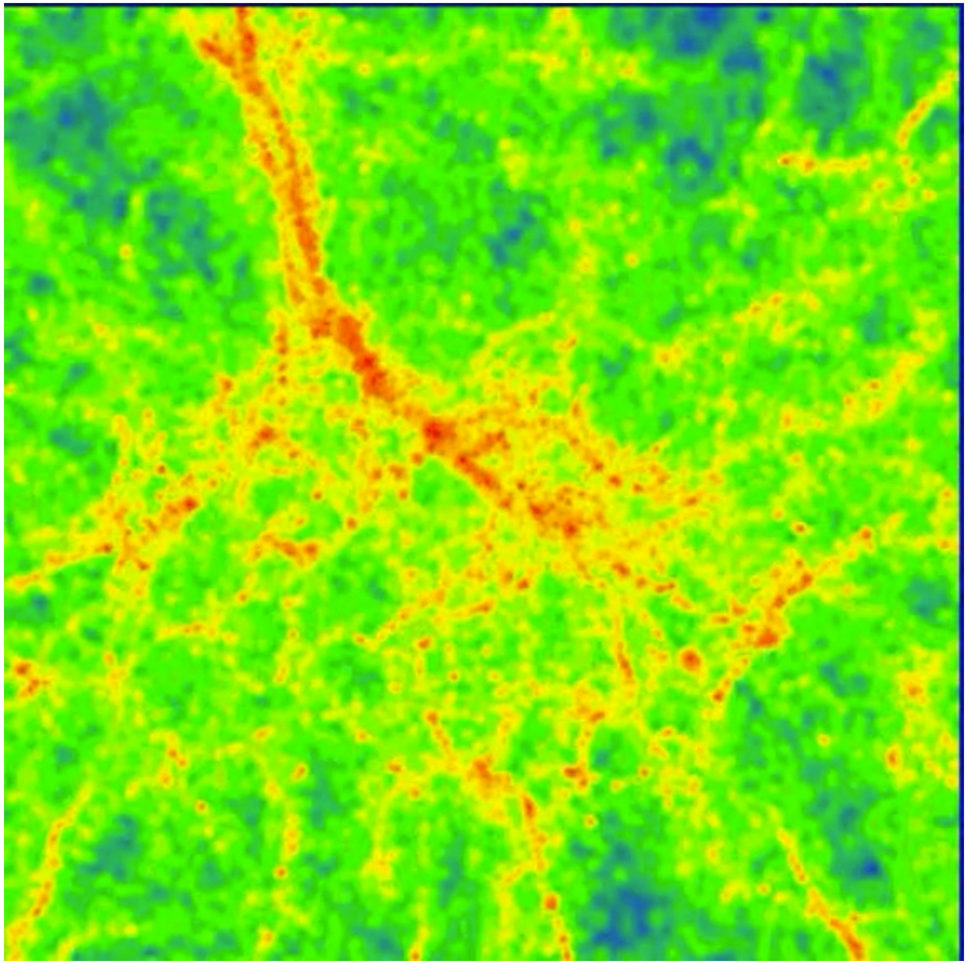

one early N-body simulation of the collapse of matter perturbations forming the cosmic web

SIMULATING COSMIC STRUCTURES

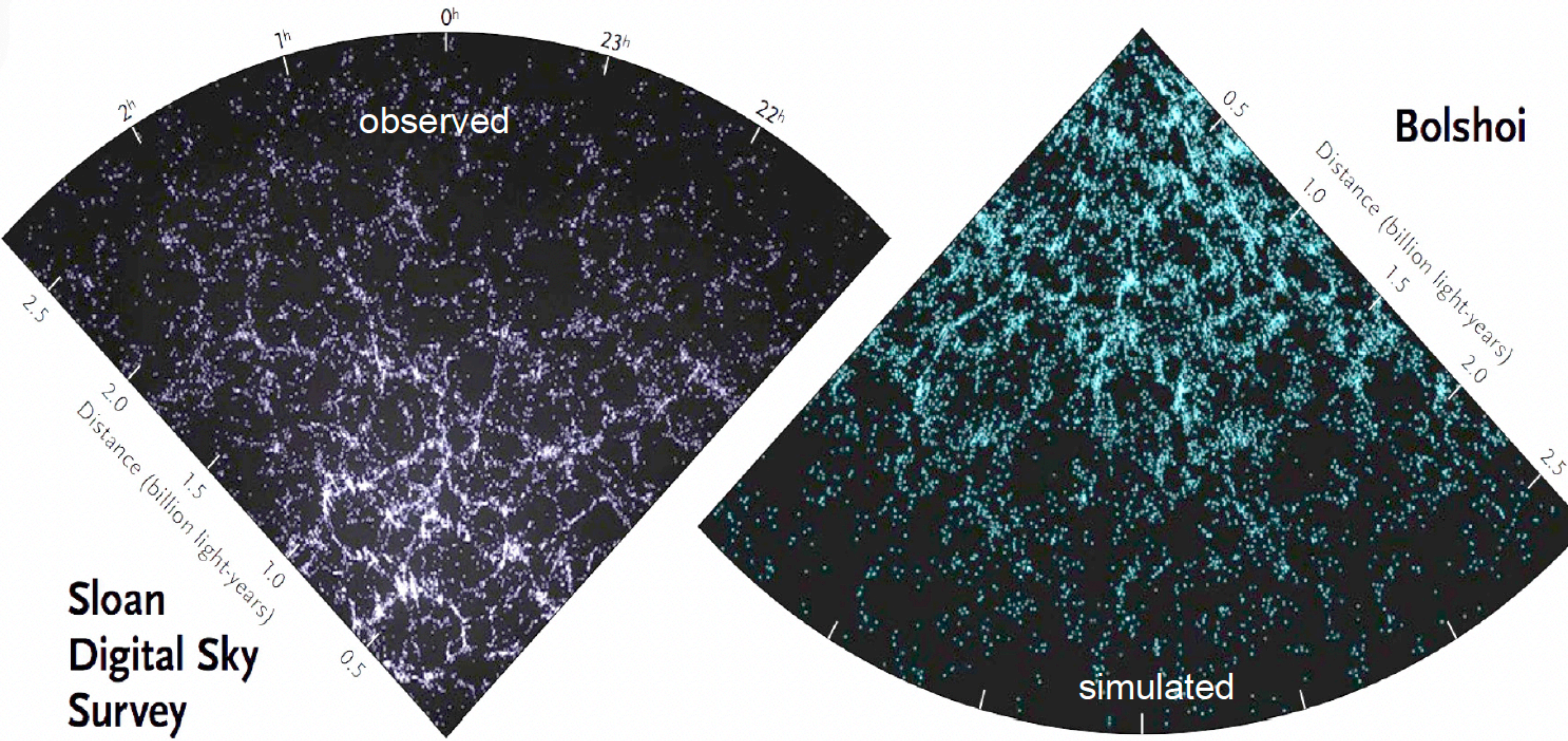

The web-like pattern of cosmic matter is one of the few actual "discoveries" made first by cosmological simulations, and later confirmed with telescopes

SIMULATING COSMIC STRUCTURES

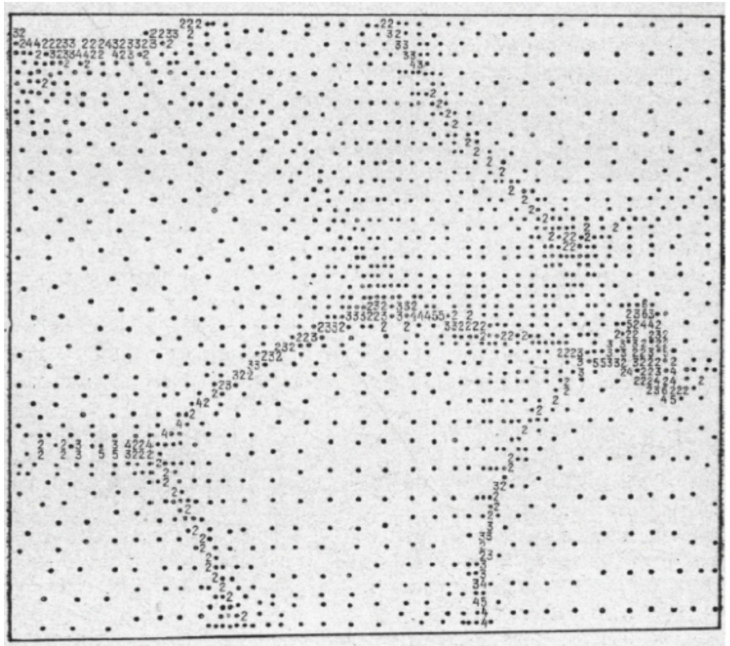

→ at the end of the '70s, many simulation using N-body methods or Zeldovich approx. consistently predicted a web-like structure for cosmic matter

→ only a few years later, the first big telescope surveys confirmed the reality of this

Chickens and blobs (1981-1982)

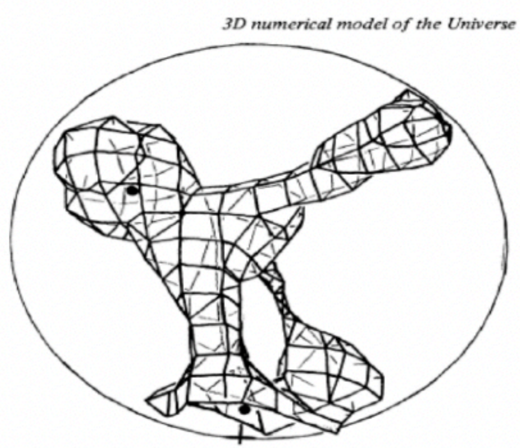

Klypin & Shandarin 1983

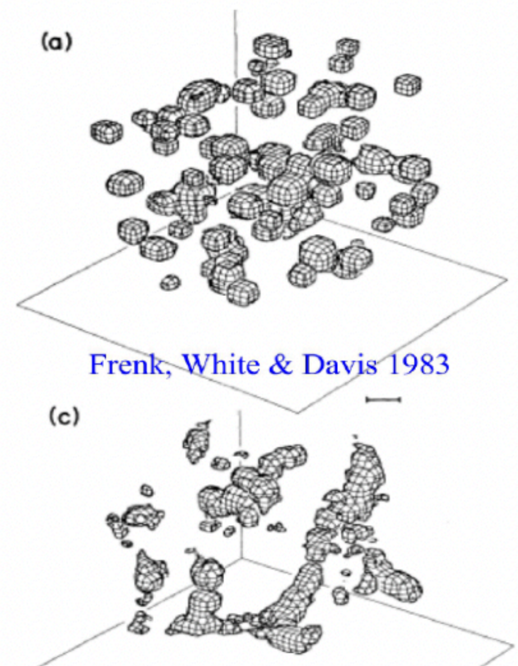

Frenk, White & Davis 1983

VOIDS, SHEETS, FILAMENTS AND CLUSTERS

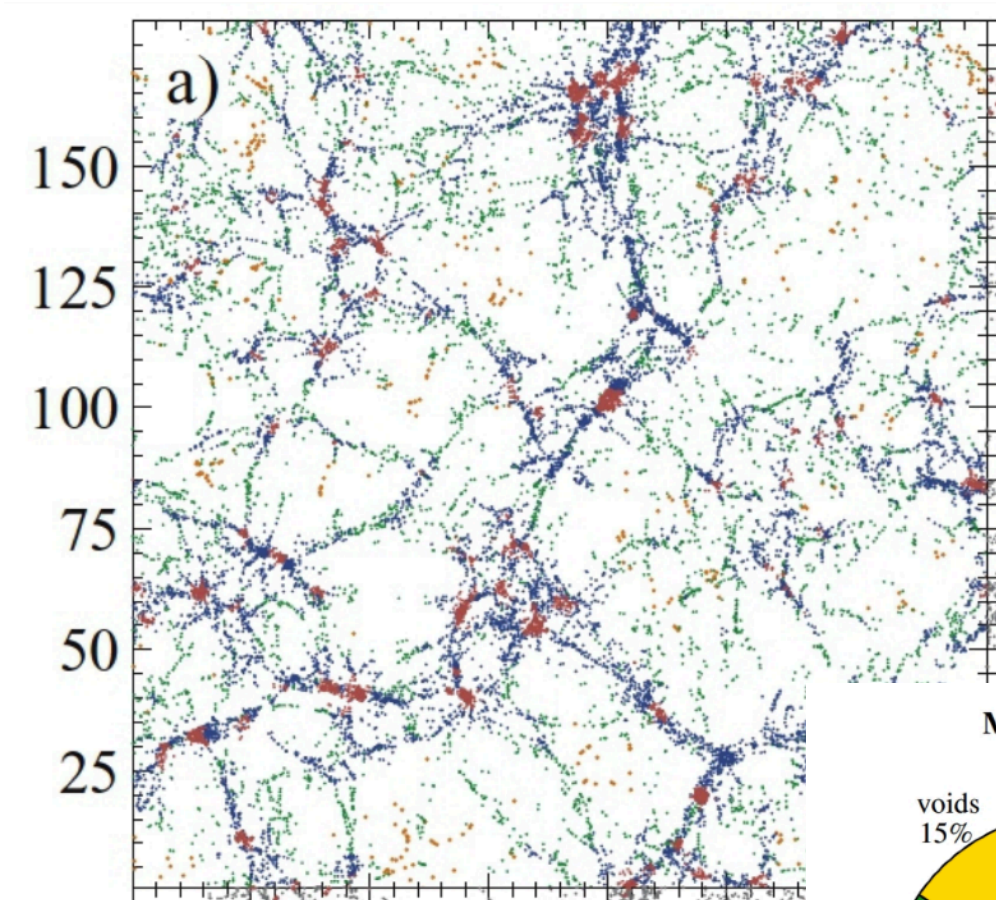

approximate overdensities of cosmic structures:

halos	$\delta \sim 10^2 - 10^4$
filaments	$\delta \sim 10$
sheets	$\delta \sim 1$
voids	$\delta \leq 0$

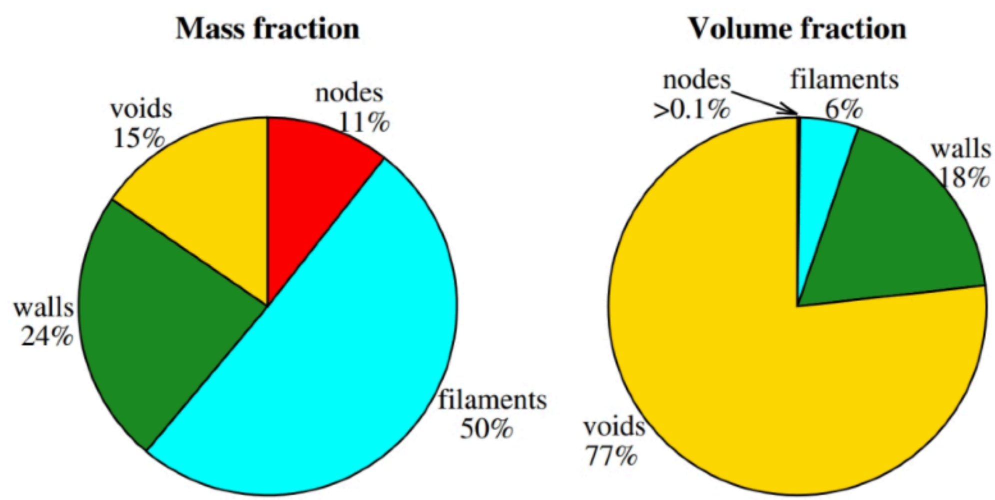

SIMULATING COSMIC STRUCTURES

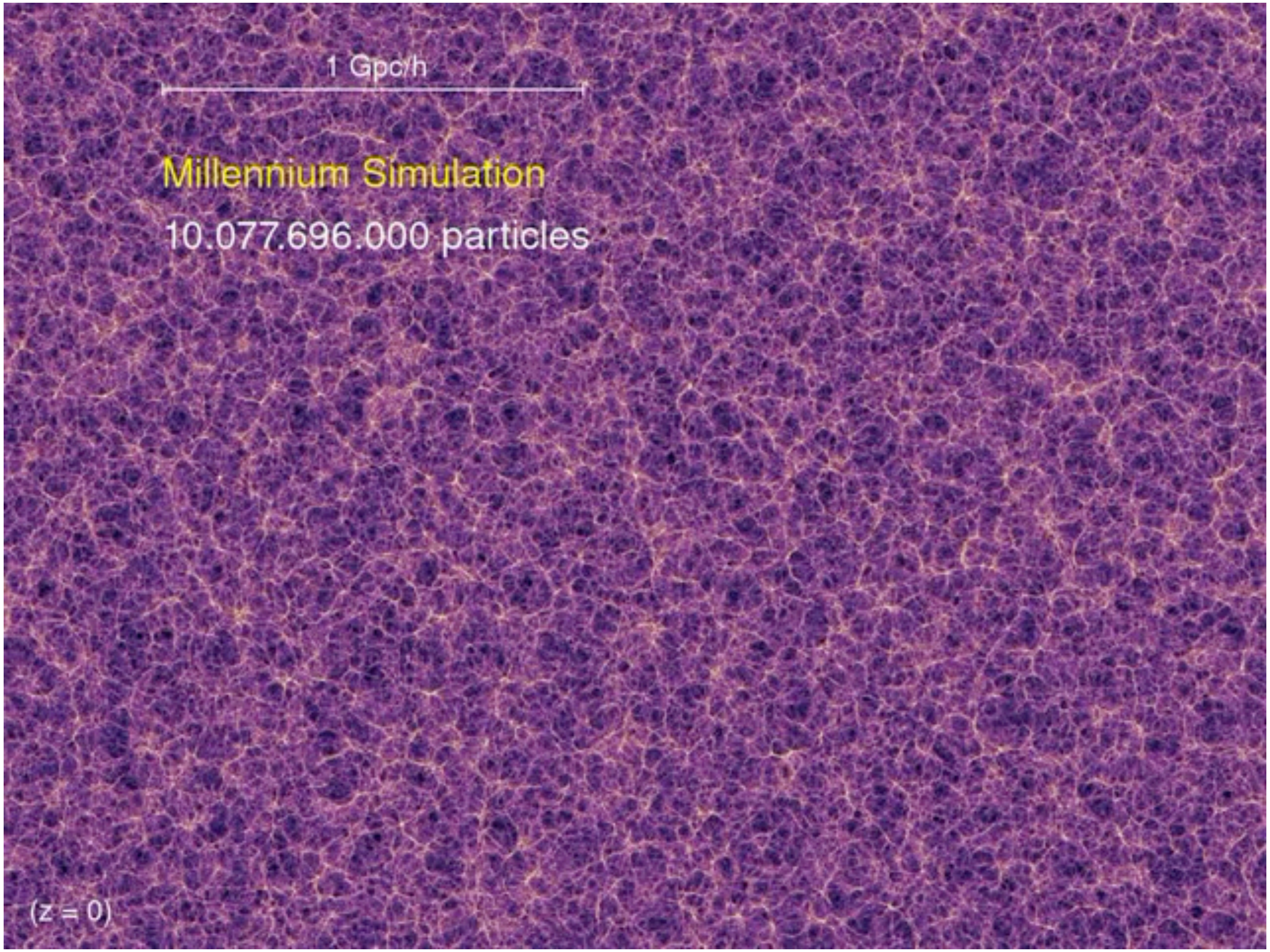

the Millennium Simulation - Springel et al 2005

SIMULATING COSMIC STRUCTURES

- All cosmological codes use the N-body approach for dark matter.
- Different particle integrators for trajectories can be used, depending on the desired accuracy of the model (e.g. “leapfrog”, “KDK”, “DKD”, Runge-Kutta etc…)
- Different gravity solvers have been developed, to make gravity computations require less than $\sim N^2$ operations as in direct summation

Hockney & Eastwood (1985): the Particle-Mesh method (PM)

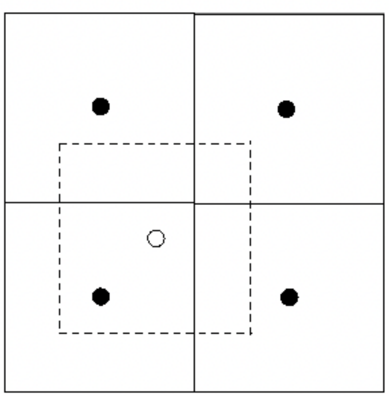

$$\sim O(N \log N)$$

Barnes & Hut (1986): the Tree method

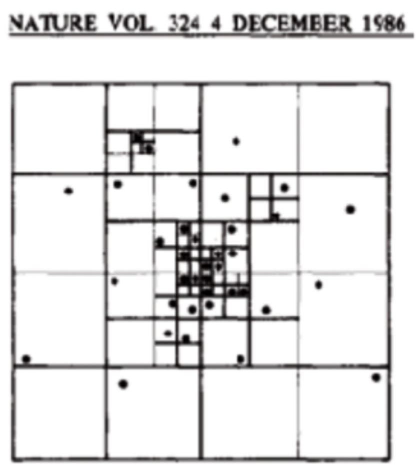

$$\sim O(N \log N)$$

Dehnen (2000): the Fast Multipole Method

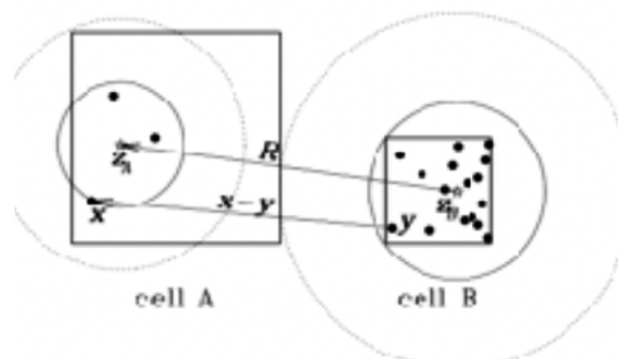

$$\sim O(N)$$

SIMULATING COSMIC STRUCTURES

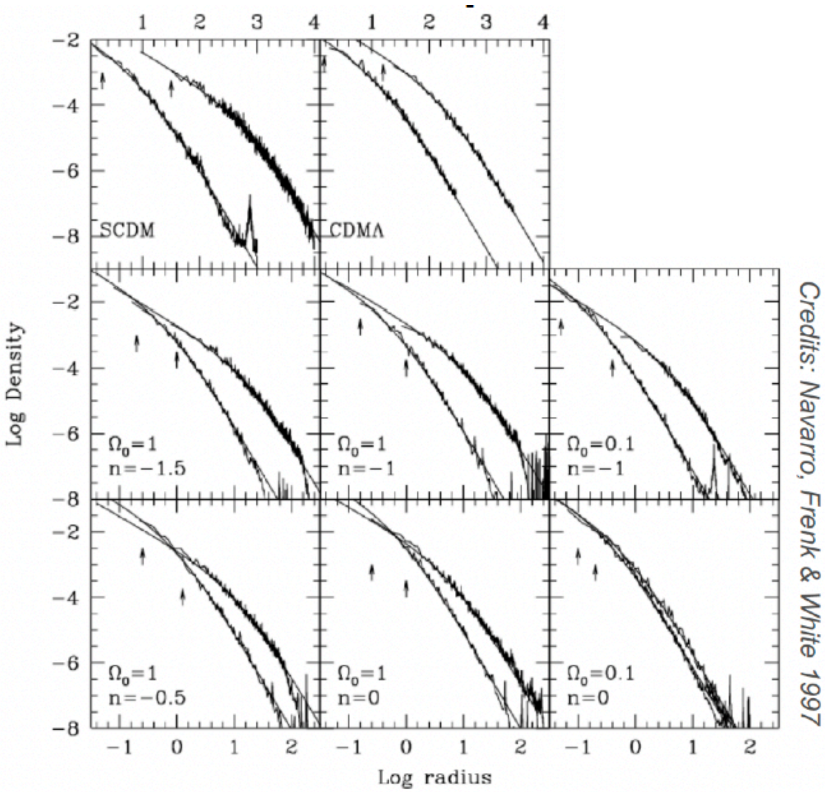

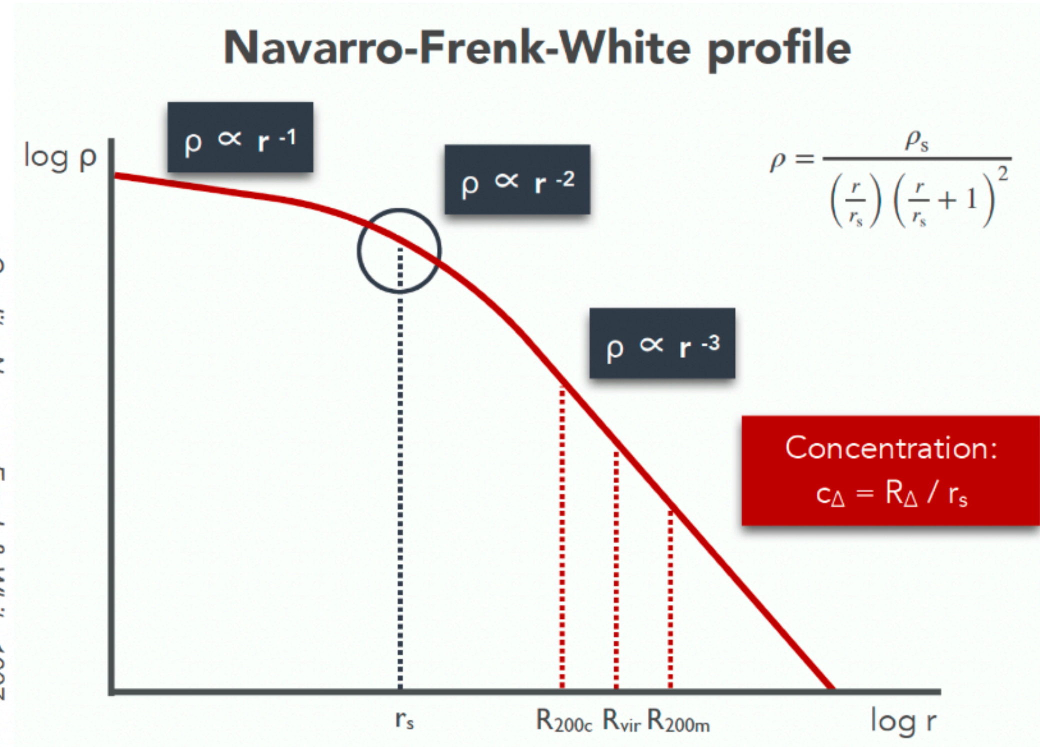

Also the analytical description of the density profile of dark matter halos - still consistent with observations on most scales- was first derived thanks to N-body dark matter simulations

SIMULATING COSMIC STRUCTURES

"BARYONS"

For "**baryons**" (=collisional ordinary matter), the minimal set of equations for their evolution is :

- velocity equation $$\frac{\partial \mathbf{v}}{\partial t} + \frac{1}{a}(\mathbf{v}\cdot\nabla)\mathbf{v} + \frac{\dot{a}}{a}\mathbf{v} = -\frac{1}{a\rho}\nabla P - \frac{1}{a}\nabla\Phi,$$
- continuity $$\frac{\partial \rho}{\partial t} + \frac{3\dot{a}}{a}\rho + \frac{1}{a}\nabla\cdot(\rho\mathbf{v}) = 0$$
- energy conservation $$\frac{\partial}{\partial t}(\rho u) + \frac{1}{a}\mathbf{v}\cdot\nabla(\rho u) = -(\rho u + P)\left(\frac{1}{a}\nabla\cdot\mathbf{v} + 3\frac{\dot{a}}{a}\right)$$

SIMULATING COSMIC STRUCTURES

"BARYONS"

velocity · expansion terms · pressure · grav.potential (gas+DM)

- velocity equation $$\frac{\partial \mathbf{v}}{\partial t} + \frac{1}{a}(\mathbf{v}\cdot\nabla)\mathbf{v} + \frac{\dot{a}}{a}\mathbf{v} = -\frac{1}{a\rho}\nabla P - \frac{1}{a}\nabla\Phi,$$

- continuity (density) $$\frac{\partial \rho}{\partial t} + \frac{3\dot{a}}{a}\rho + \frac{1}{a}\nabla\cdot(\rho\mathbf{v}) = 0$$

- energy conservation $$\frac{\partial}{\partial t}(\rho u) + \frac{1}{a}\mathbf{v}\cdot\nabla(\rho u) = -(\rho u + P)\left(\frac{1}{a}\nabla\cdot\mathbf{v} + 3\frac{\dot{a}}{a}\right)$$

internal energy

(+ radiation, heating, chemistry…**magnetic fields & cosmic rays**)

SIMULATING COSMIC STRUCTURES

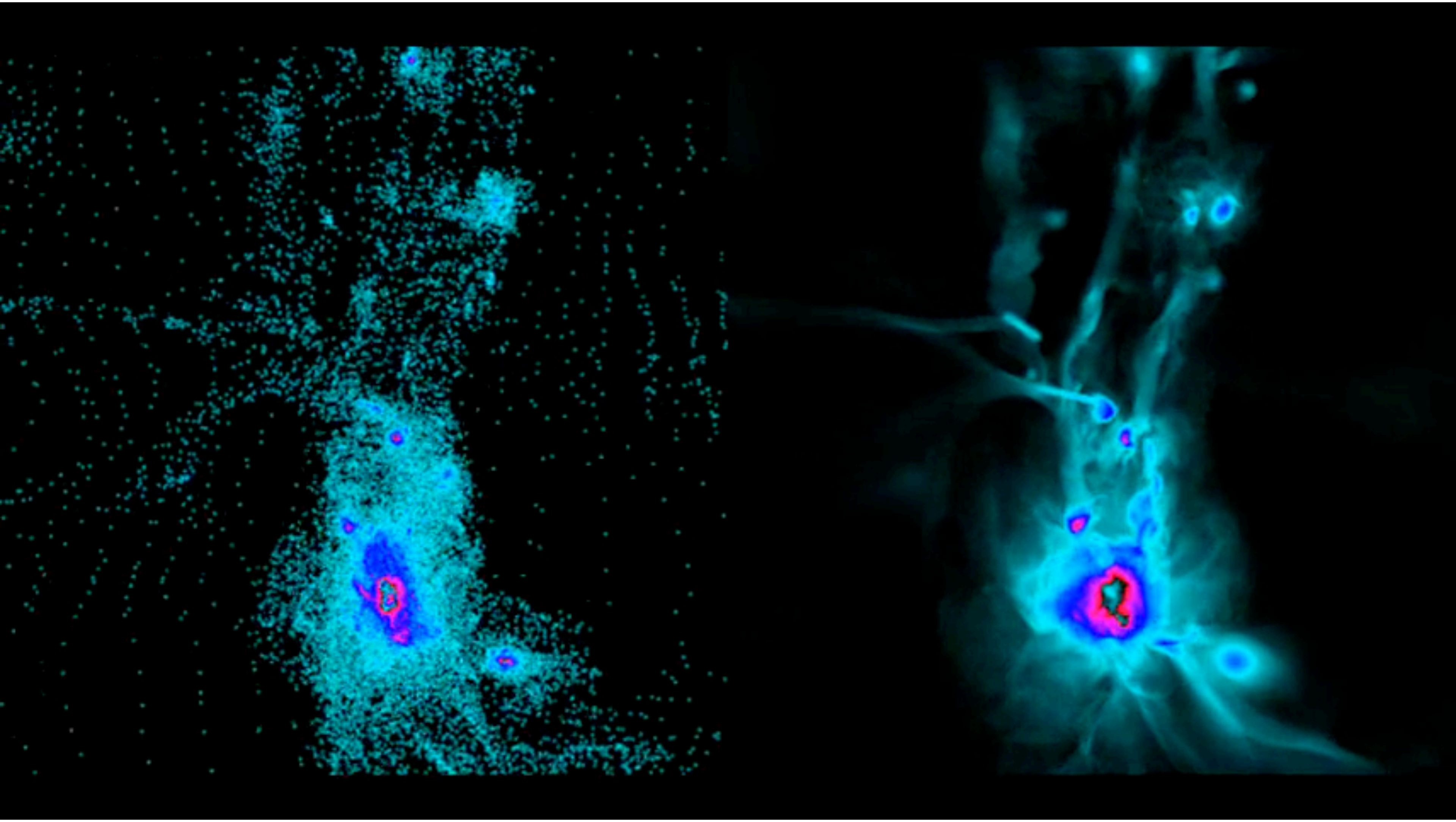

dark matter baryons

TWO BASIC METHODS

Eulerian	Lagrangian	“**S**moothed **P**article **H**ydrodynamics”

discretize space

representation on a mesh
(volume elements)

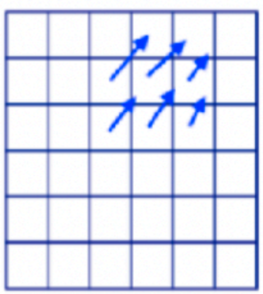

principle advantage:

high accuracy (shock capturing), low numerical viscosity

discretize mass

representation by fluid elements
(particles)

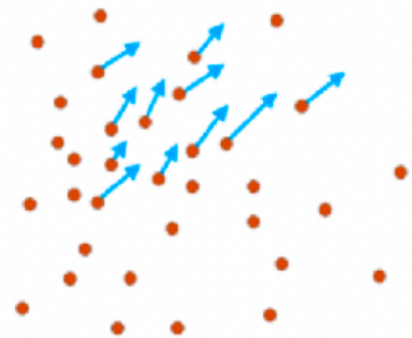

principle advantage:

resolutions adjusts automatically to the flow

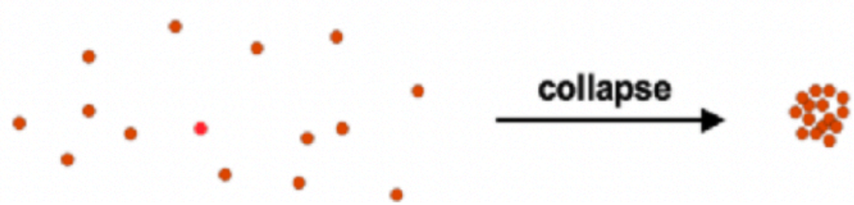

Credits: V.Springel

TWO BASIC METHODS

Eulerian

from fluid variables (u_n) to **reconstruction** at the cell interfaces

3 different possible reconstruction methods

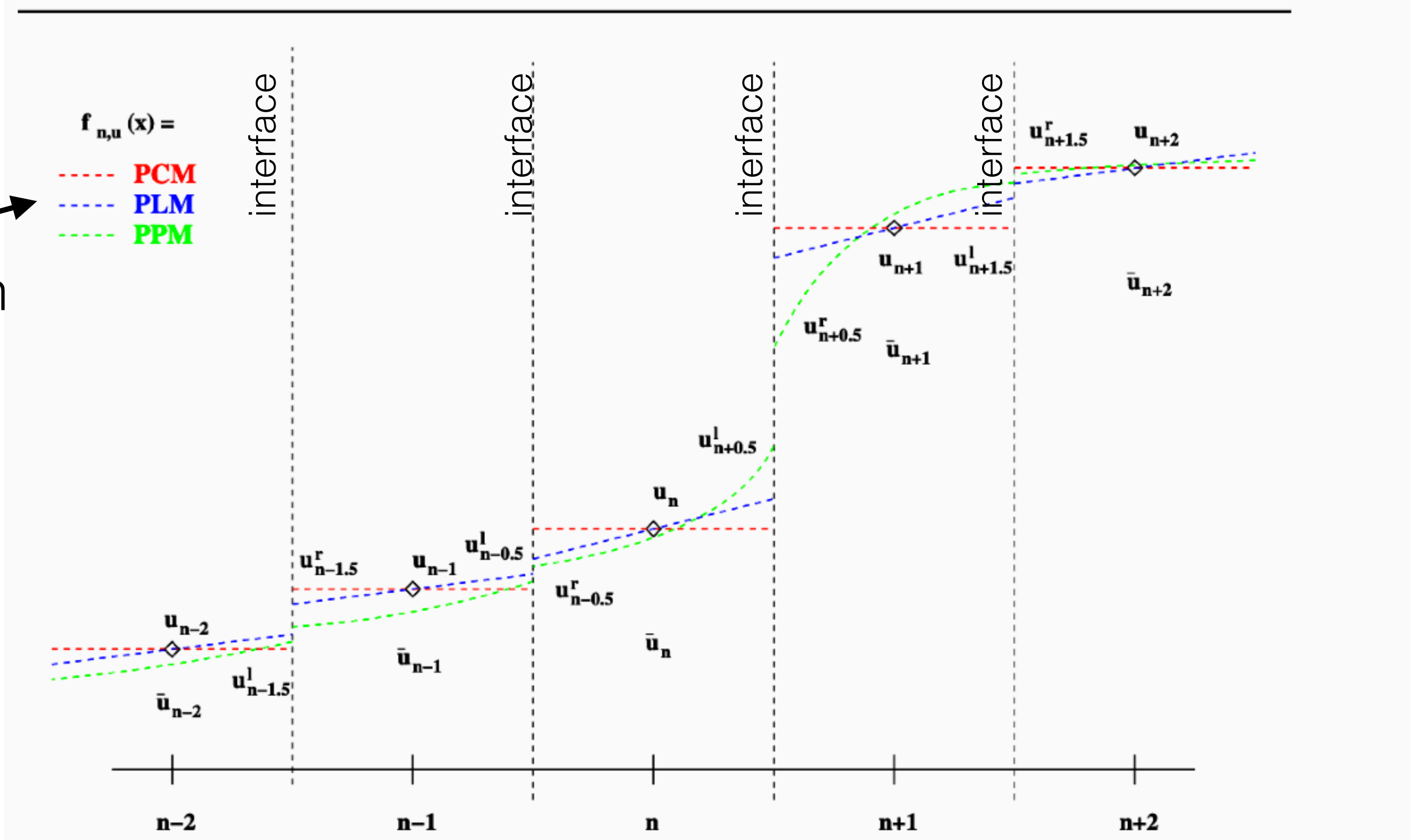

Fig. 9 Reconstruction of the principal variables (u_n) on the grid using different methods, like *piecewise constant* (PCM), *piecewise linear* (PLM) or *piecewise parabolic* (PPM). The reconstruction scheme then allows one to calculate cell averages ($\bar{u}_n$) as well as the left and right-hand sided values on the cell boundaries ($u^l_{n\pm0.5}$,$u^r_{n\pm0.5}$).

TWO BASIC METHODS

Eulerian

from fluid variables (u_n) to **reconstruction** at the cell interfaces

3 different possible reconstruction methods

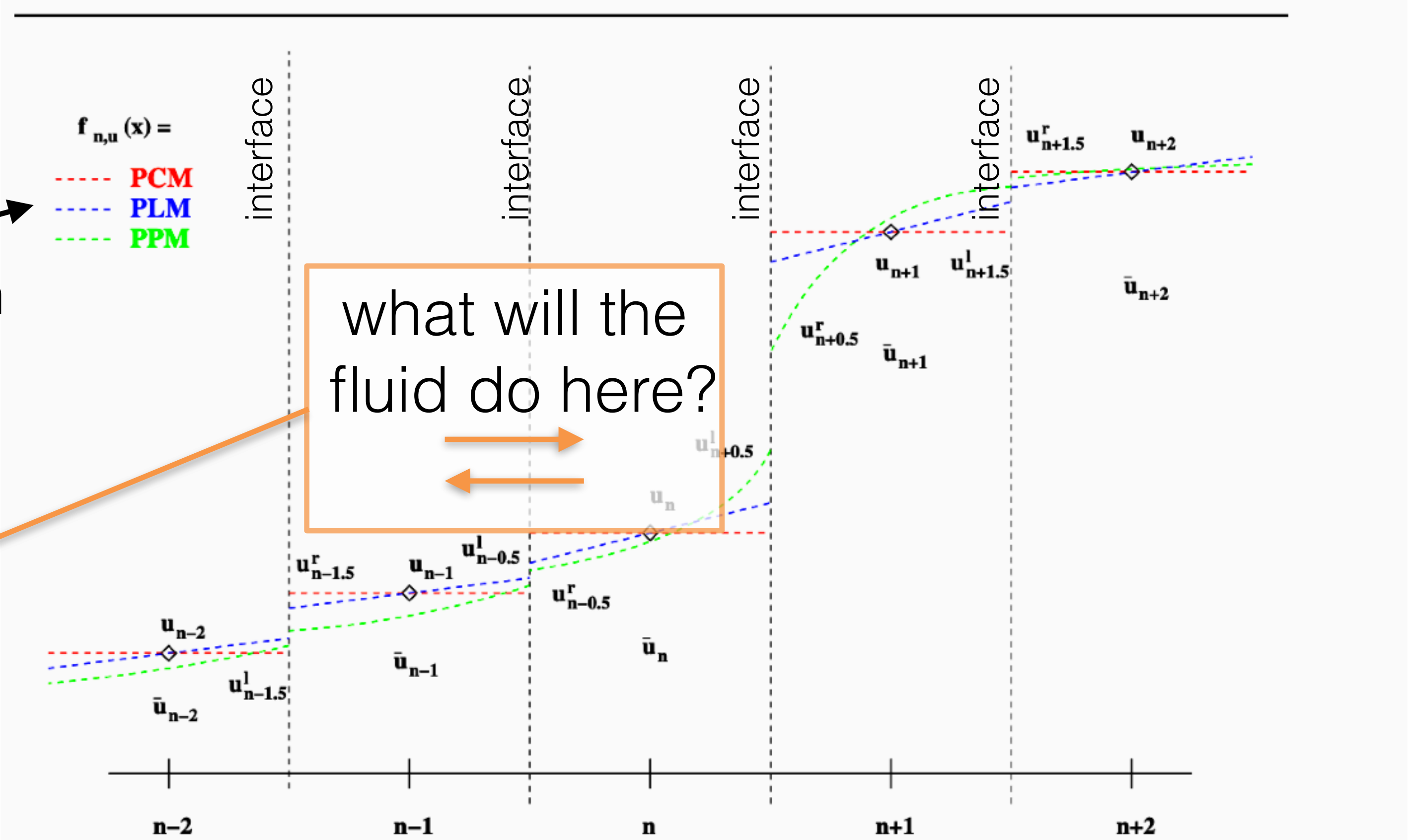

we have to solve for the **FLUX** across cells → "Riemann Solver"

Fig. 9 Reconstruction of the principal variables (u_n) on the grid using different methods, like *piecewise constant* (PCM), *piecewise linear* (PLM) or *piecewise parabolic* (PPM). The reconstruction scheme then allows one to calculate cell averages ($\bar{u}_n$) as well as the left and right-hand sided values on the cell boundaries ($u^l_{n\pm0.5}$, $u^r_{n\pm0.5}$).

TWO BASIC METHODS

Eulerian

Riemann solvers:

iterative algorithm to compute the evolution of fluid quantities at the interfaces, based on physical solutions from standard hydro-dynamics.

The fluid values at the cell centre are updated using all 3D fluxes given by the Riemann solver.

This directly ensures that ordinary matter is evolved based on physical solutions

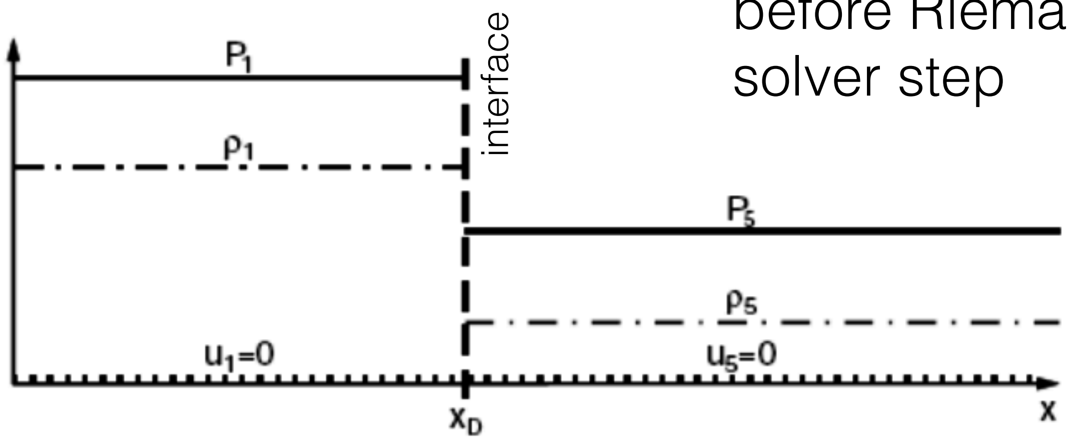

before Riemann solver step

TWO BASIC METHODS

Eulerian

Riemann solvers:

iterative algorithm to compute the evolution of fluid quantities at the interfaces, based on <u>physical solutions</u> from standard hydro-dynamics.

The fluid values at the cell centre are updated using all 3D fluxes given by the Riemann solver.

<u>This directly ensures that ordinary matter is evolved based on physical solutions</u>

before Riemann solver step

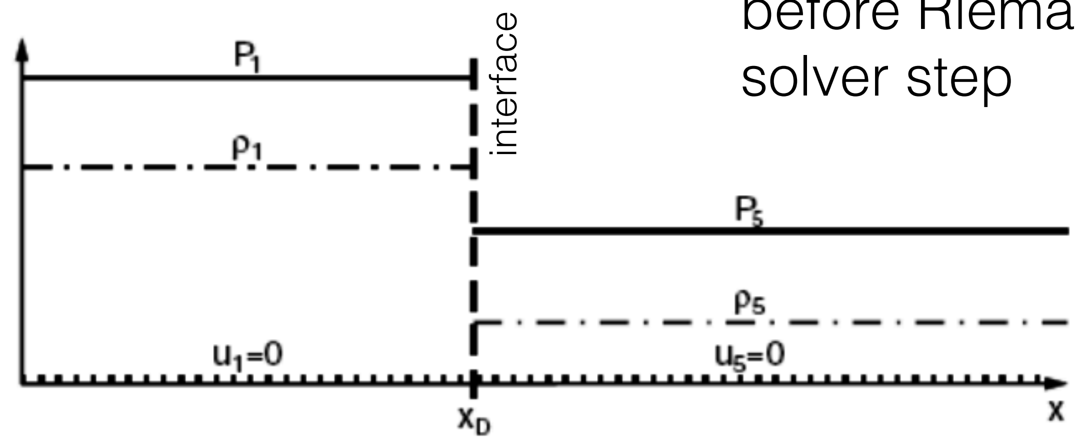

after Riemann solver step

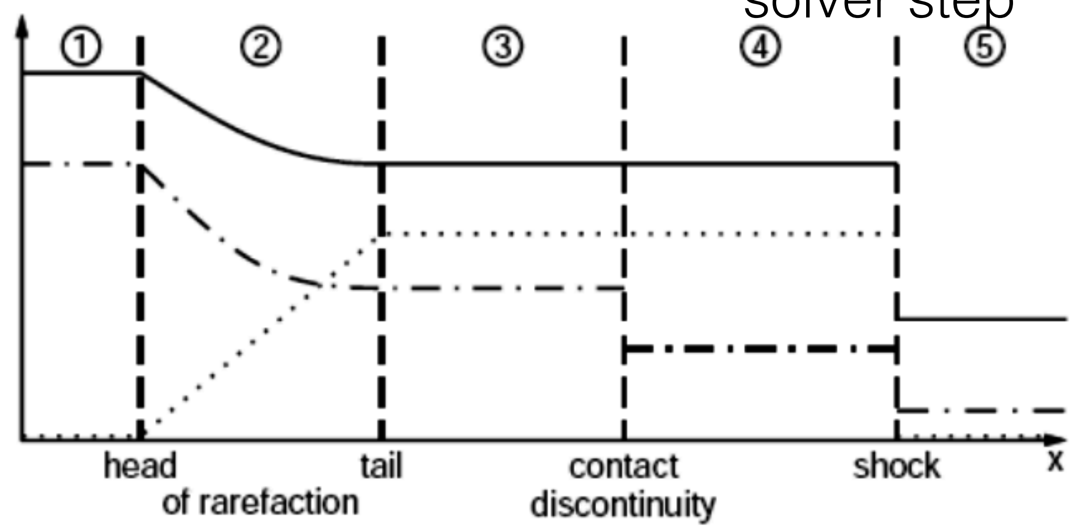

TWO BASIC METHODS

Smoothed Particle Hydrodynamics

A discrete set of N particles is used to sample a continuous fluid distribution

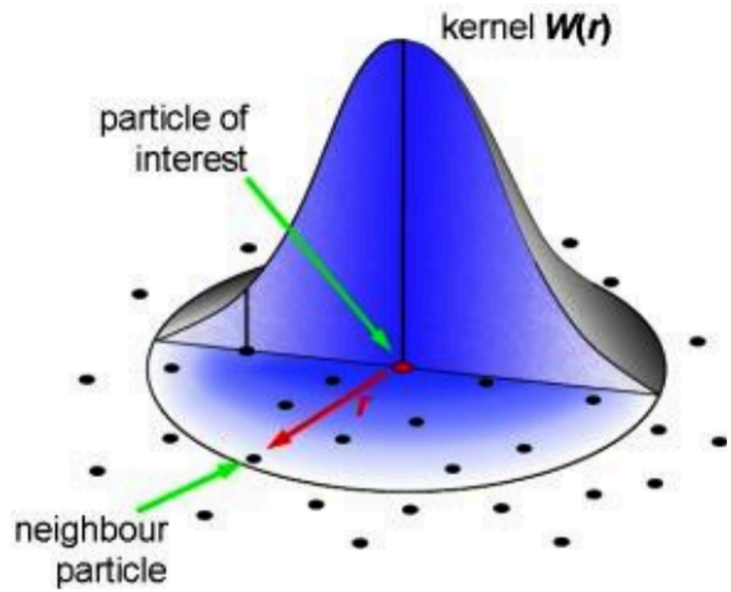

Fluid quantities are estimated by convolving a set of "neighbouring" particles $\sim O(10^2)$ with a kernel function $\langle A_i \rangle = \langle A(\mathbf{x}_i) \rangle = \sum_j \frac{m_j}{\rho_j} A_j W(\mathbf{x_i} - \mathbf{x_j}, h)$

The momentum equation becomes:

$$\frac{\mathrm{d}u_i}{\mathrm{d}t} = \frac{1}{2} \sum_j m_j \left(\frac{P_j}{\rho_j^2} + \frac{P_i}{\rho_i^2} + \Pi_{ij} \right) (\mathbf{v}_j - \mathbf{v}_i) \nabla_i W(\mathbf{x_i} - \mathbf{x_j}, h).$$

TWO BASIC METHODS

Smoothed Particle Hydrodynamics

To make an N-body method collisional, we enforce some viscous dissipation for nearby particles (otherwise they will cross each other!)

In SPH, this was traditionally done with an adjustable artificial viscosity (μ_{ab}), which is on for approaching particles ($\nabla \cdot v < 0$)

$$\left(\frac{\mathrm{d}\boldsymbol{v}_a}{\mathrm{d}t}\right)_{\mathrm{AV}} = -\sum_b m_b \frac{-\alpha \bar{c}_{ab}\mu_{ab} + \beta \mu_{ab}^2}{\bar{\rho}_{ab}} \nabla_a W_a$$

where

$$\mu_{ab} \equiv \begin{cases} \frac{\boldsymbol{v}_{ab}\cdot \boldsymbol{r}_{ab}}{r_{ab}^2 + \epsilon h^2} & \boldsymbol{v}_{ab}\cdot \boldsymbol{r}_{ab} < 0; \\ 0 & \boldsymbol{v}_{ab}\cdot \boldsymbol{r}_{ab} \geq 0, \end{cases}$$

This ensures the right energy dissipation at shocks, but also introduces unphysical viscosity

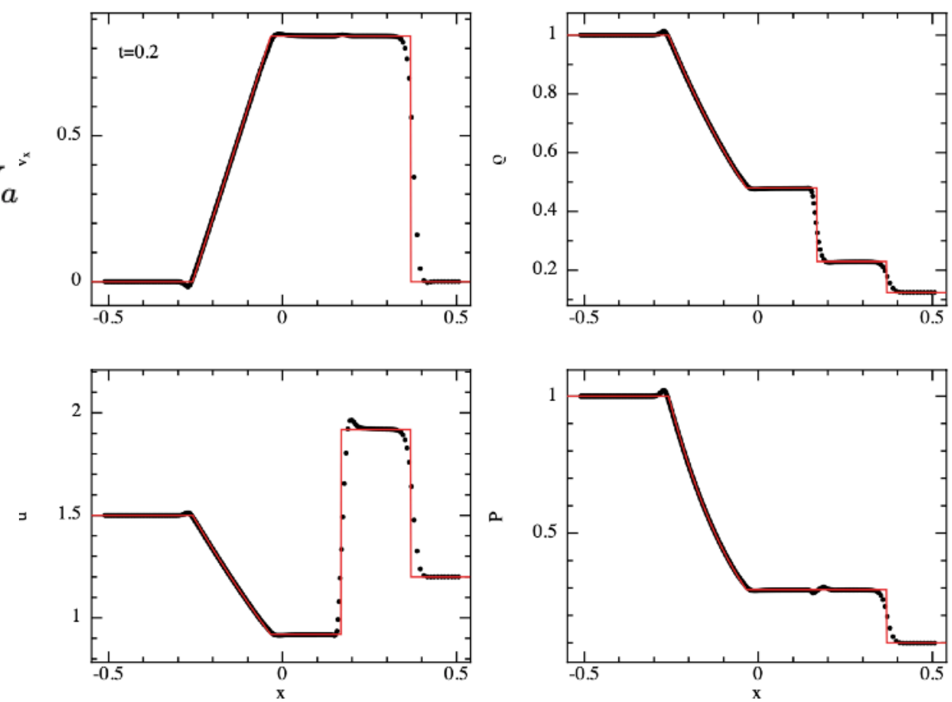

Fig. 1. 1D Sod shock tube computed using artificial viscosity with constant coefficients $\alpha = 1$ and $\beta = 2$.

TWO BASIC METHODS

Eulerian

discretize space

representation on a mesh
(volume elements)

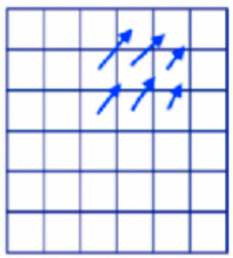

Lagrangian

“**S**moothed **P**article **H**ydrodynamics”

discretize mass

representation by fluid elements
(particles)

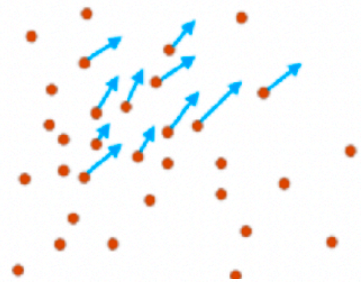

PROS:

+ Fair sampling of all volume
+ Physical hydro solutions from Riemann solver
+ Captures well shocks

CONS

- non Galileian invariant
- had problems in conserving angular momentum

PROS:

+ Fair sampling of mass
+ Automatically provides higher resolution where matter clusters
+ Conserves angular momentum

CONS

- artificial viscosity
- difficult to accurately follow sharp hydro features

WHICH METHOD IS BEST?

Tests of 1D shocks vs analytical solution

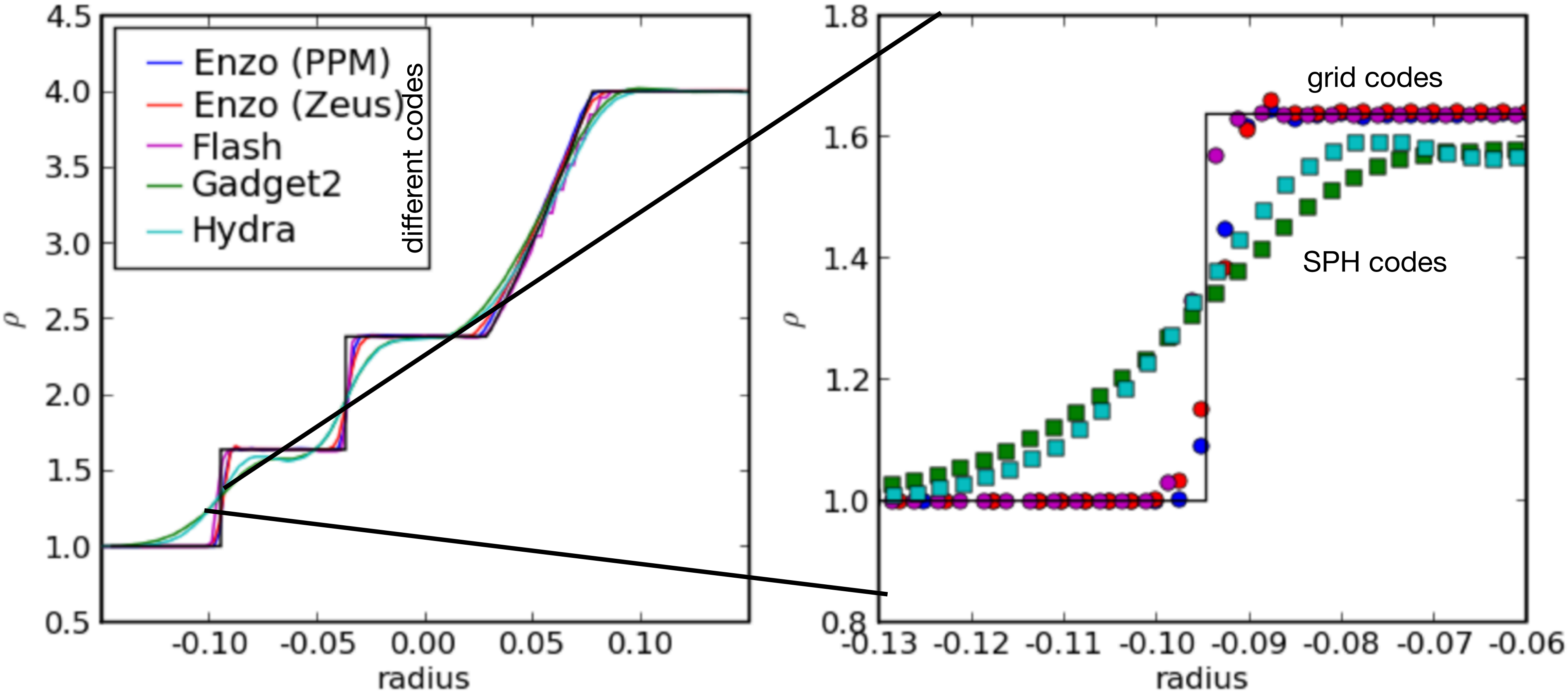

old SPH codes always provide smoother reconstruction of shocks (+spurious generation of entropy)

Tasker et al. 2009

WHICH METHOD IS BEST? SOME EARLY CODE COMPARISON

The "Santa Barbara" comparison project (Frenk+99)

12 codes to simulate the evolution of the same (?) cluster

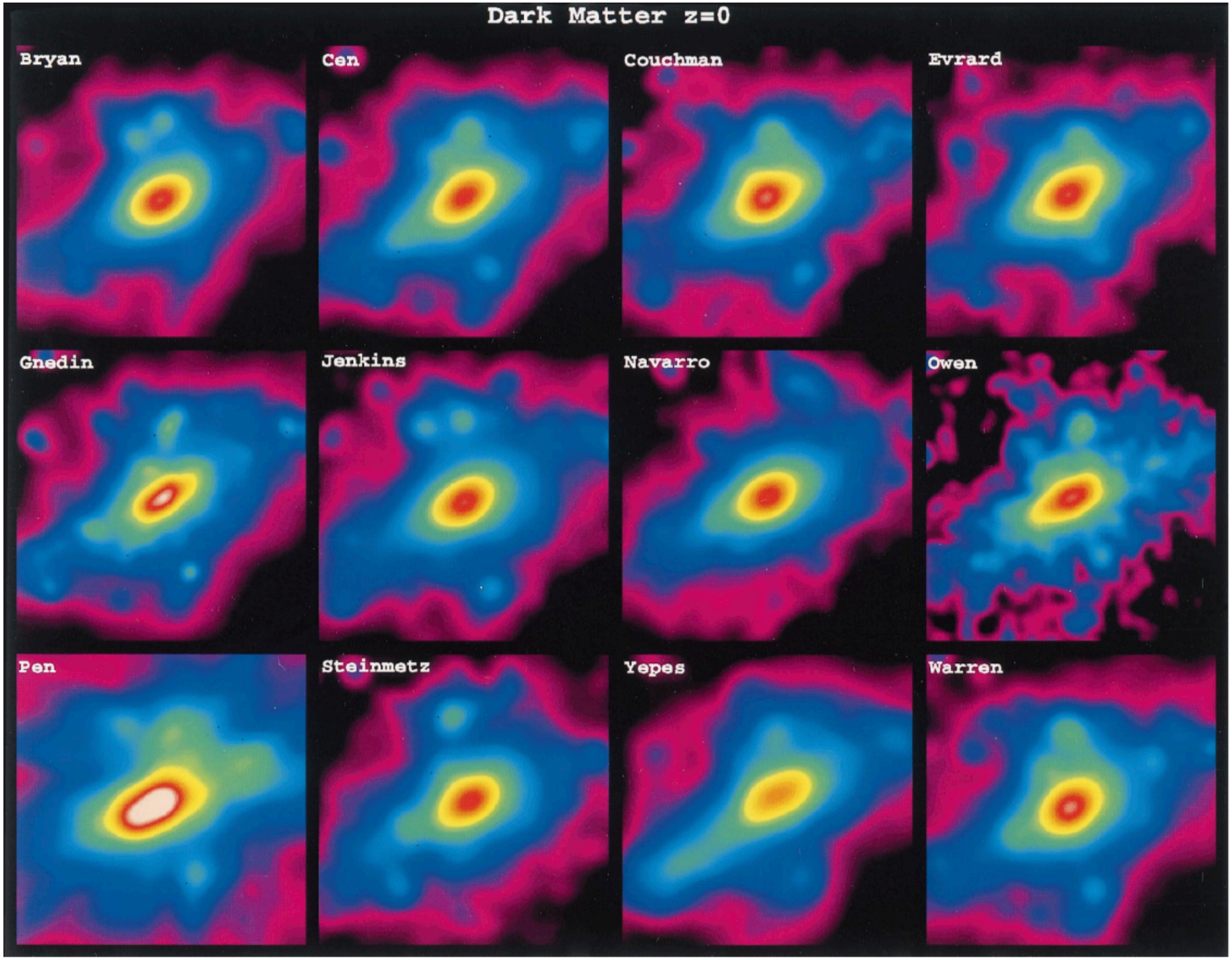

Dark matter density: quite similar (gravity is "easy"!)

All codes used a similar N-body approach

WHICH METHOD IS BEST? SOME EARLY CODE COMPARISON

The "Santa Barbara" comparison project (Frenk+99)

12 codes to simulate the evolution of the same (?) cluster

Gas matter density:
quite different.

Differences in hydro solver and time stepping makes simulations inconsistent

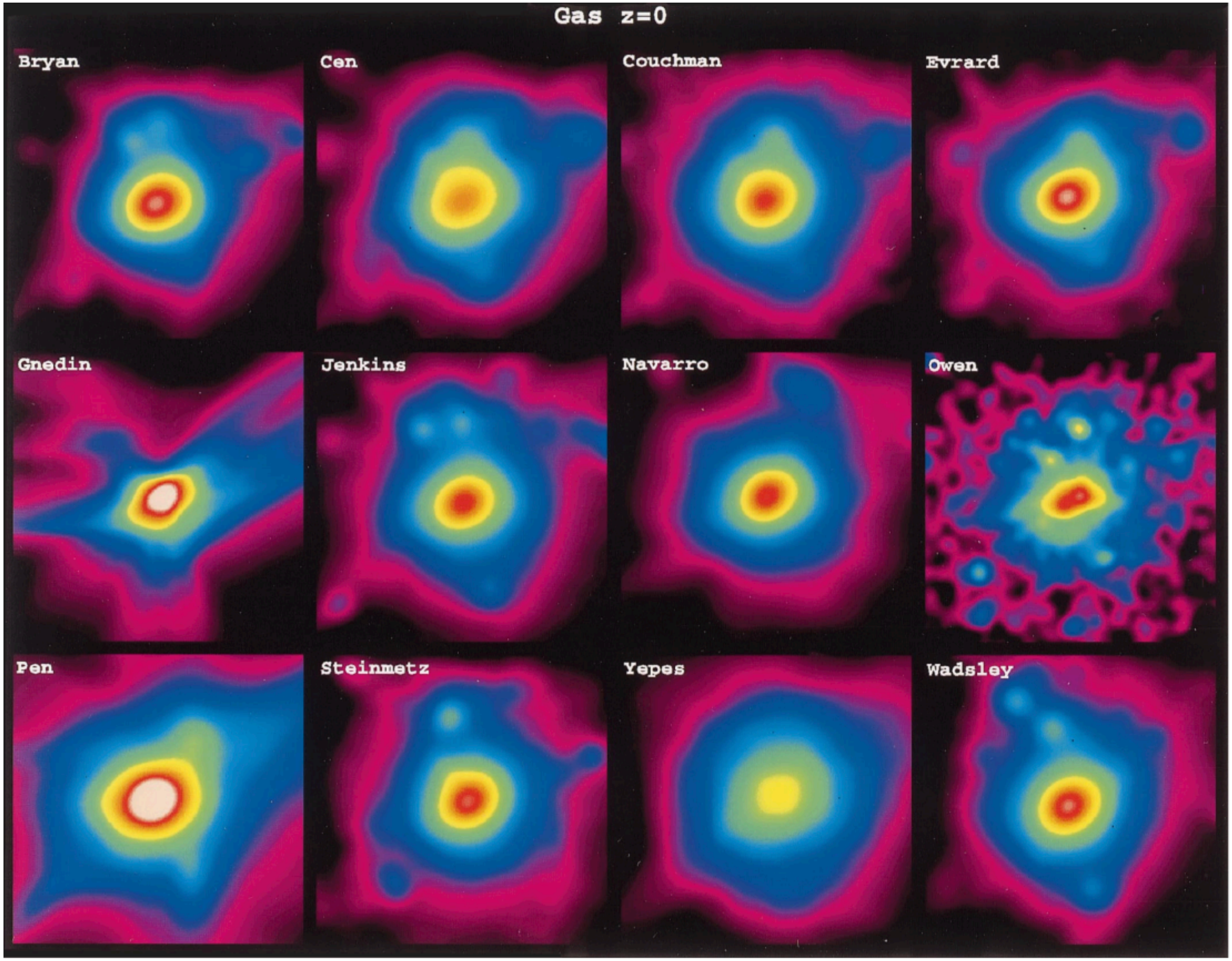

WHICH METHOD IS BEST? SOME EARLY CODE COMPARISON

The “Santa Barbara” comparison project (Frenk+99)

12 codes to simulate the evolution of the same (?) cluster

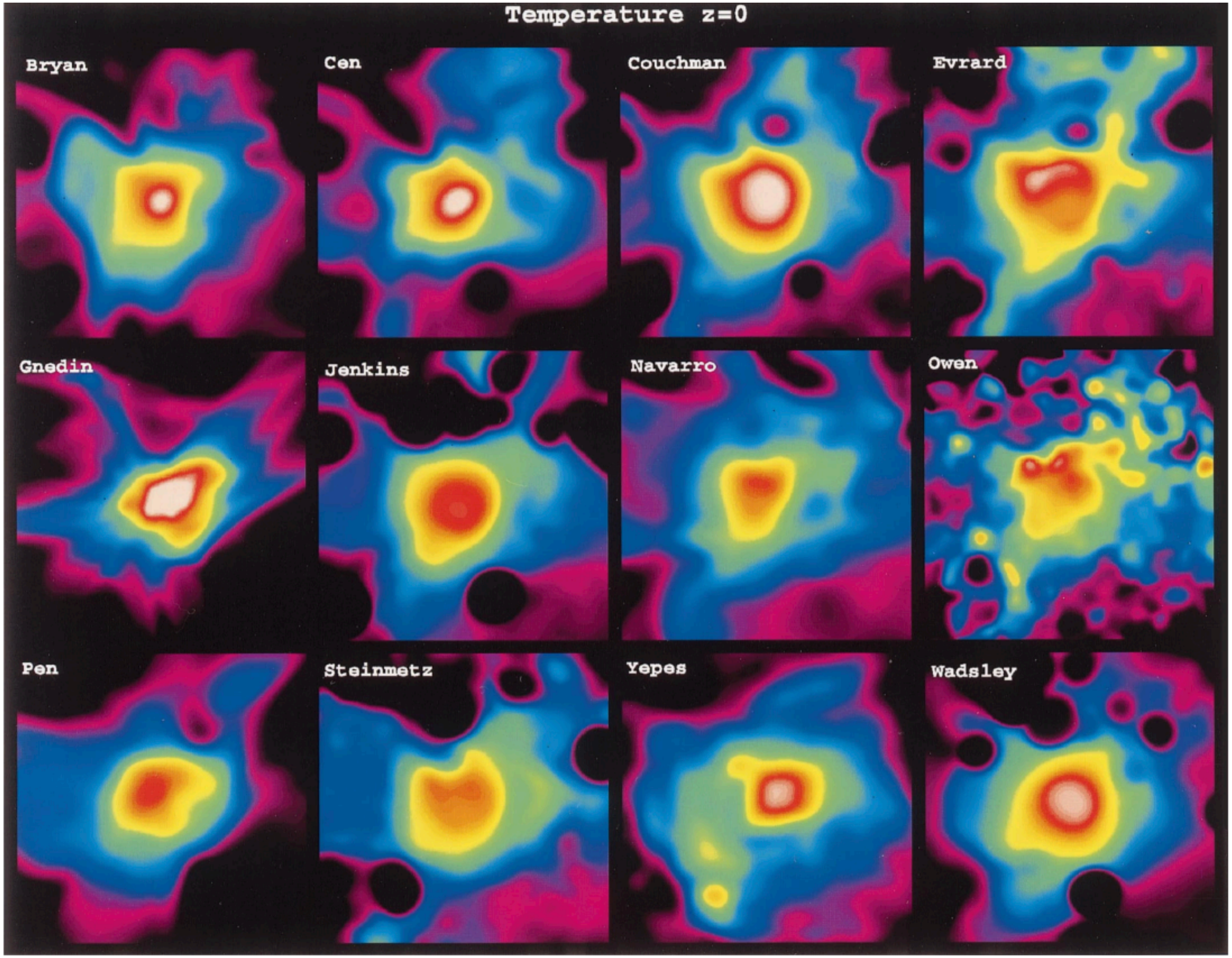

Gas matter temperature: very different.

Further differences in the thermodynamics of gas

WHICH METHOD IS BEST? SOME EARLY CODE COMPARISON

The "Santa Barbara" comparison project (Frenk+99)

12 codes to simulate the evolution of the same (?) cluster

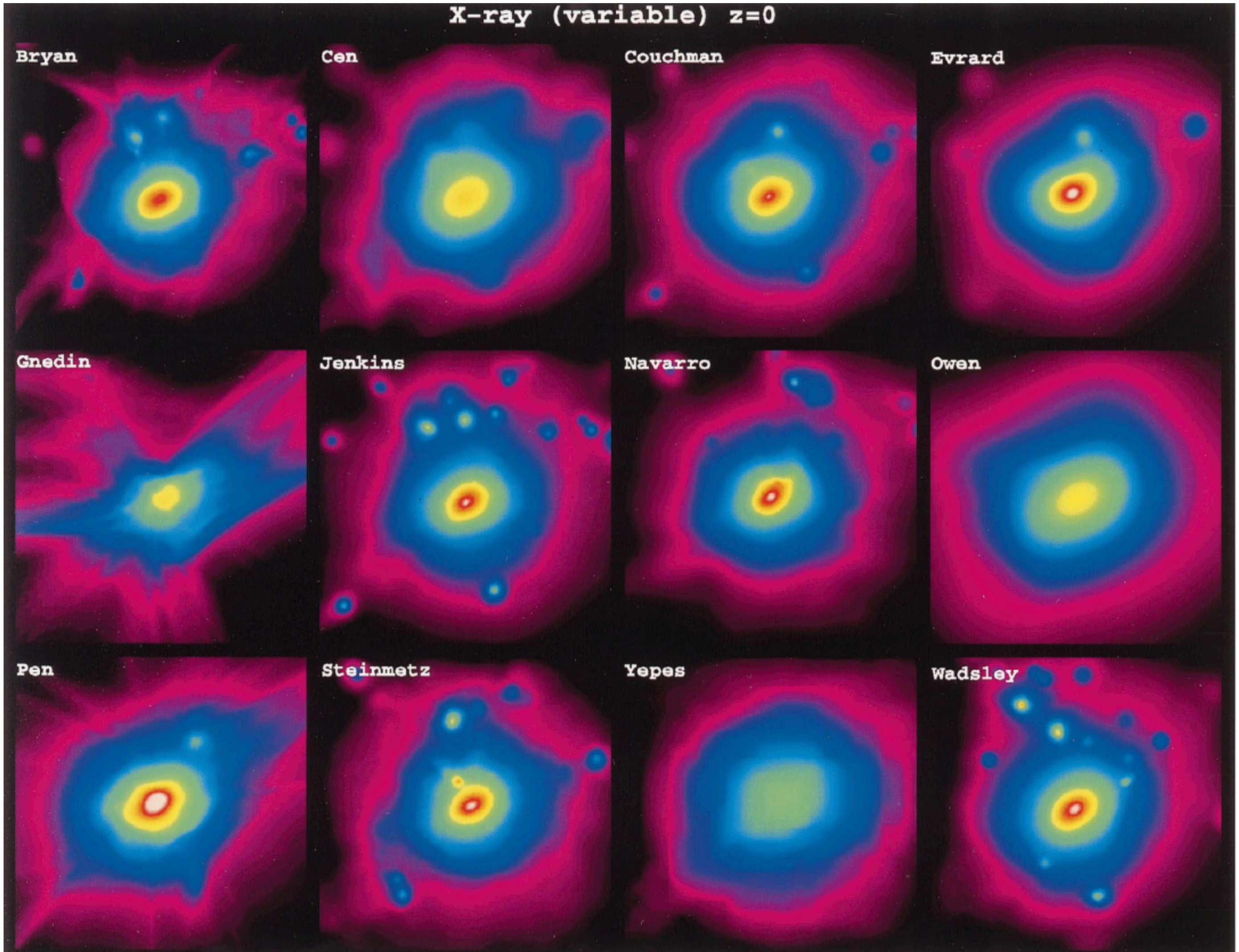

X-ray emission: very different.

how can we observationally validate theoretical predictions, if numerics introduces so many differences?

WHICH METHOD IS BEST? SOME EARLY CODE COMPARISON

Simulated binary merger: the colored points represent: SPH particles from two halos (left, GADGET) and tracer particles on top of an Eulerian simulation with the same two halos (right, FLASH)

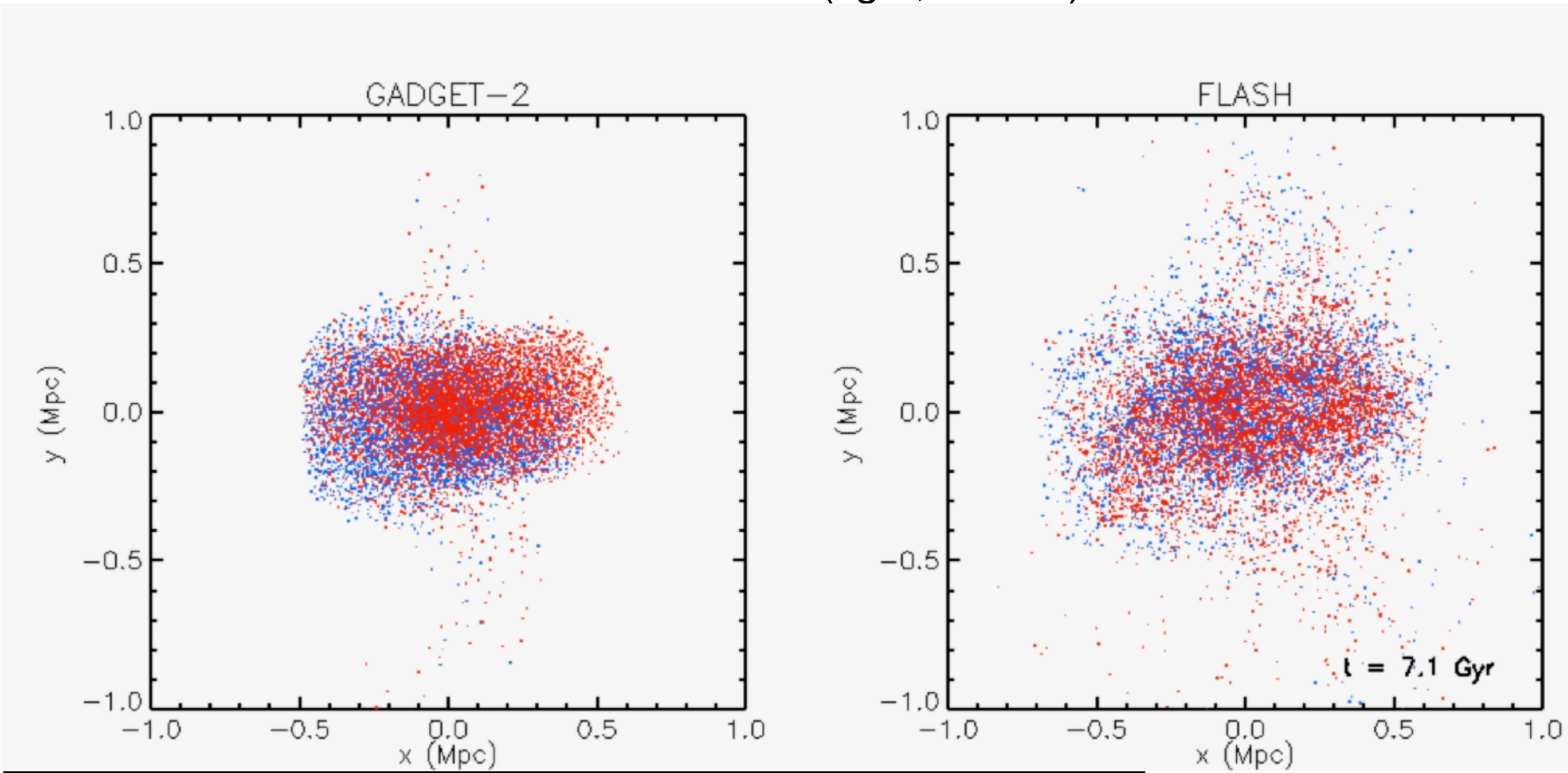

Depending on the method, very different level of “mixing” between the two cluster. Particles settle do difference place in the two cases!

Mitchell+2009

WHICH METHOD IS BEST? SOME EARLY CODE COMPARISON

Grid simulation (FLASH): more mixing between clusters, gas in the centre of the newly formed cluster has high entropy

SPH simulation (Gadget): less mixing between clusters, gas in the centre of the newly formed cluster has low entropy

energy dissipation and entropy mixing are different in the two methods

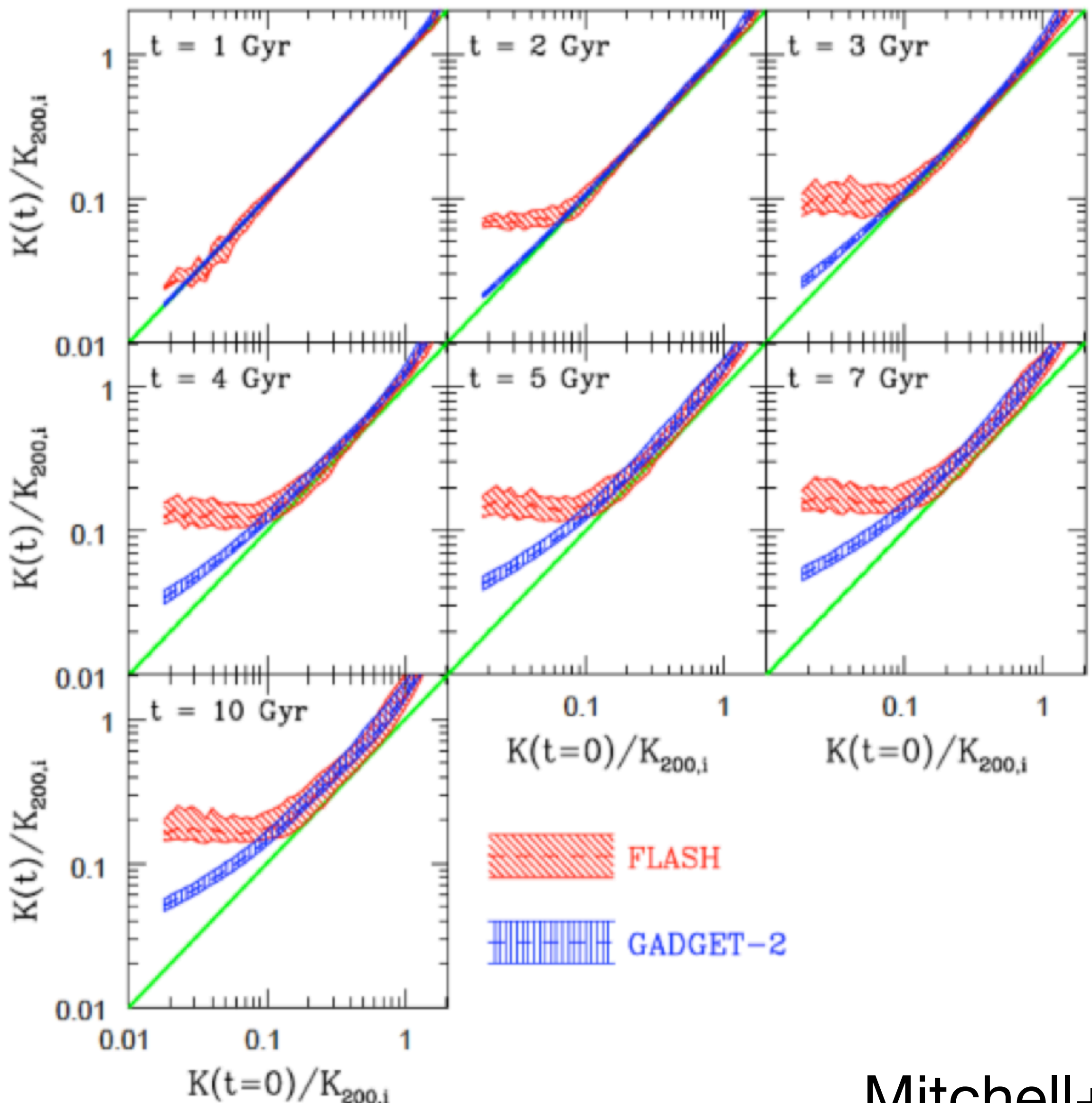

Mitchell+2009

WHICH METHOD IS BEST? SOME EARLY CODE COMPARISON

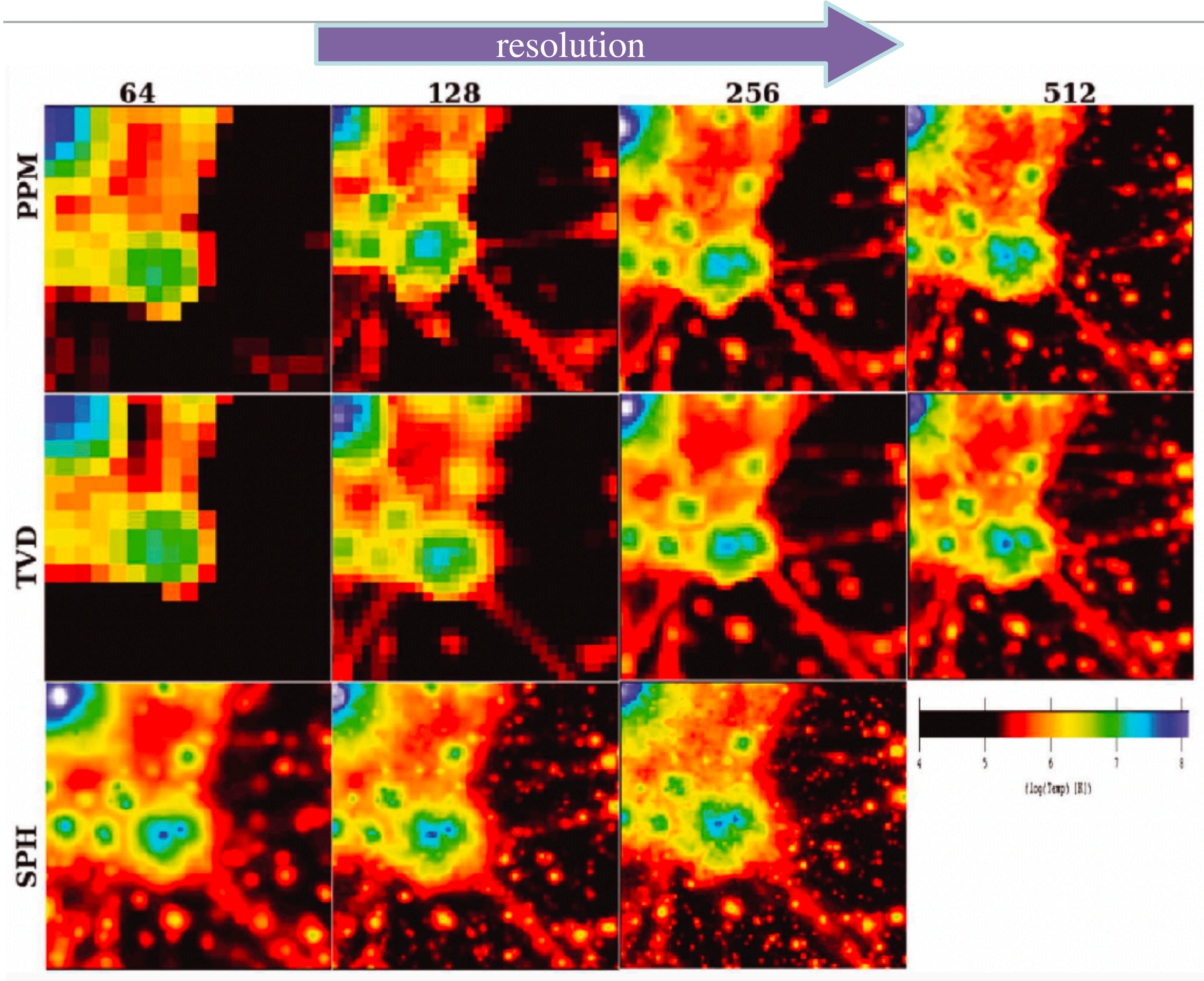

Overall good convergence of thermal gas distribution

WHICH METHOD IS BEST? AN EARLY CODE COMPARISON

Map of shocks (displayed: Mach number) :
very different distributions

grid simulation, PPM solver | grid simulation, SPH solver | grid simulation, TVD solver

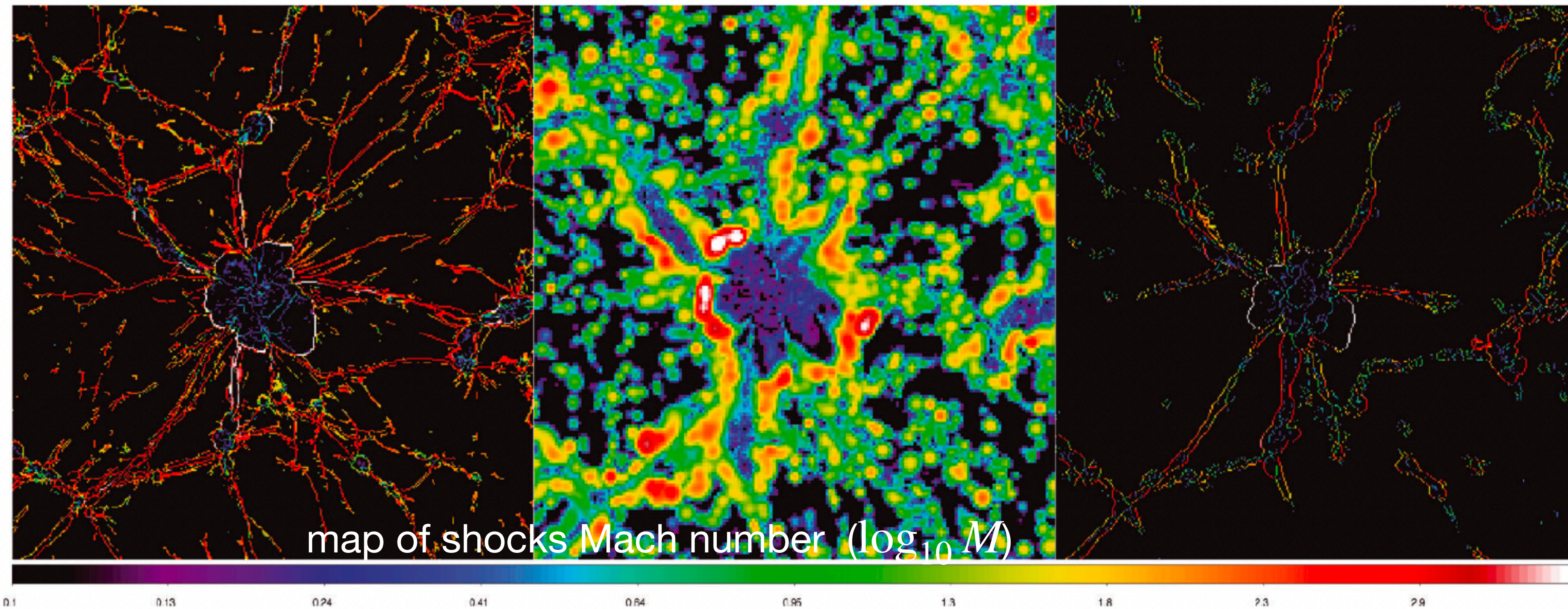

Vazza et al. 2012

WHICH METHOD IS BEST? AN EARLY CODE COMPARISON

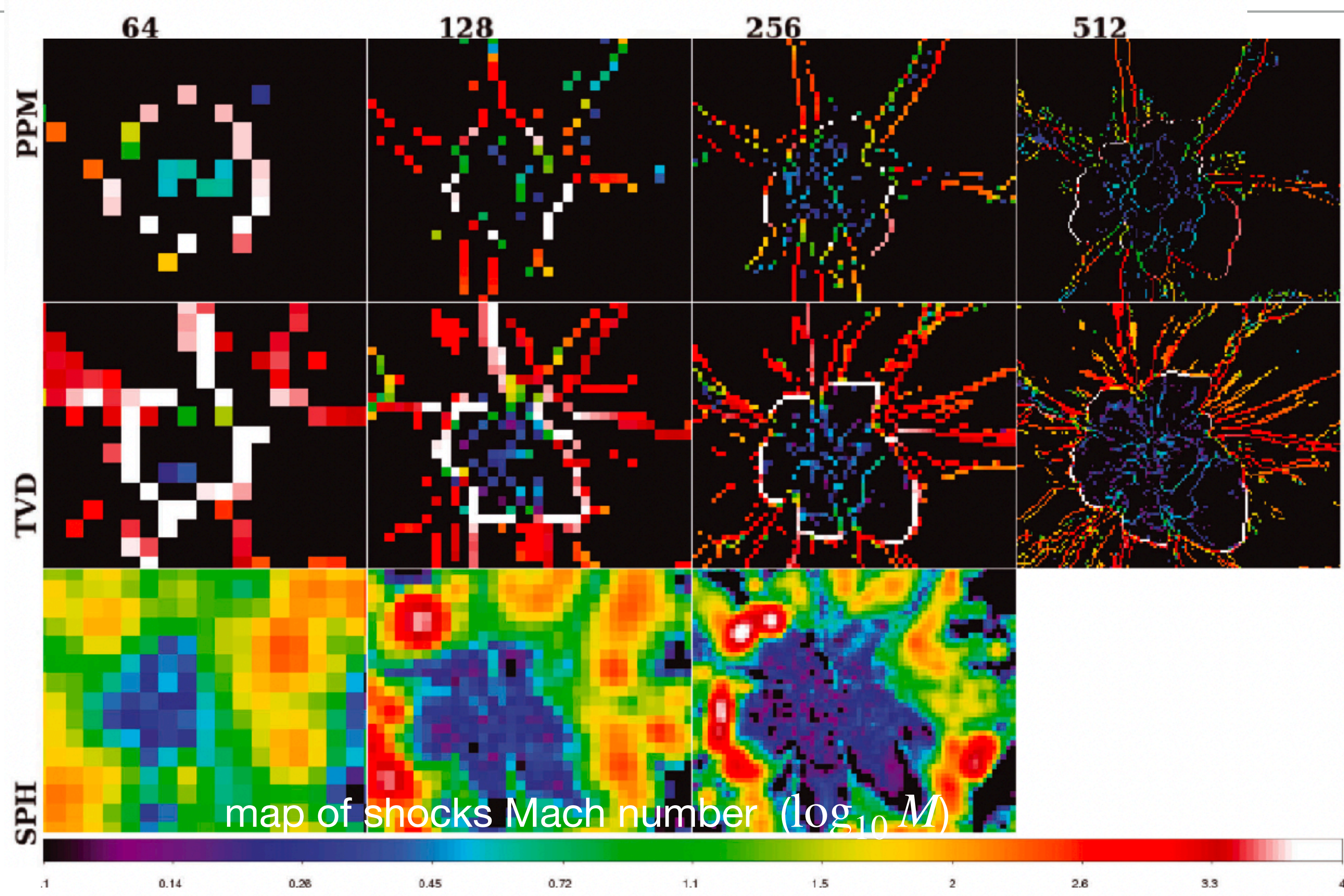

No clear convergence with resolution:
grid codes produce sharper shocks, SPH clumpier shocks.
How can we predict cosmic ray acceleration?

Vazza et al. 2012

WHICH METHOD IS BEST?   ADVECTION PROBLEMS

<u>**Galileian invariance**</u>: the solution to a physical problem does not depend on the reference frame. Ideally, a simulation should get the same solution even if its reference frame moves. But in grid methods, the errors in advection may dominates physical velocity differences and <u>instabilities are damped by numerical diffusion:</u> solutions are not galileian invariant!

Rayleigh-Taylor instabilities in a grid simulation: moving vs static mesh.

Springel 2010

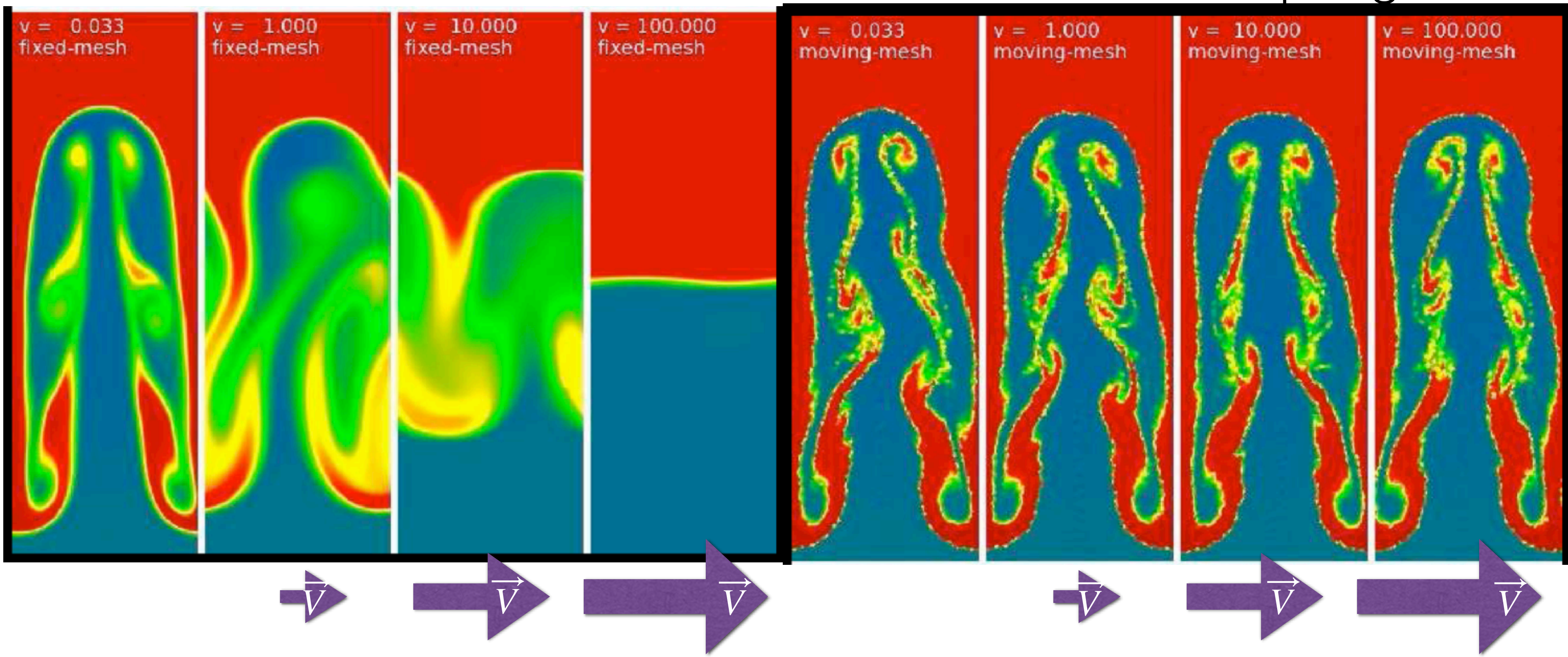

This motivated the development of “moving mesh” codes. e.g. AREPO and GIZMO

WHICH METHOD IS BEST?

Effective numerical diffusion coefficient in Eulerian solvers

cell resolution

$$\alpha = \frac{1}{2} v \Delta x (1 - |c|),$$

constant <1

advection velocity

Eulerian codes needs to decrease α as much as possible. If $|v| > 0$, then Δx should be as small as possible, i.e. increasing resolution

…it's expensive!

Robertson+2011

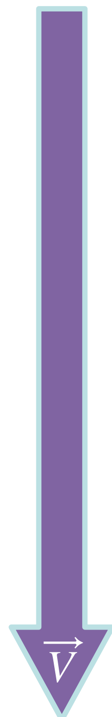

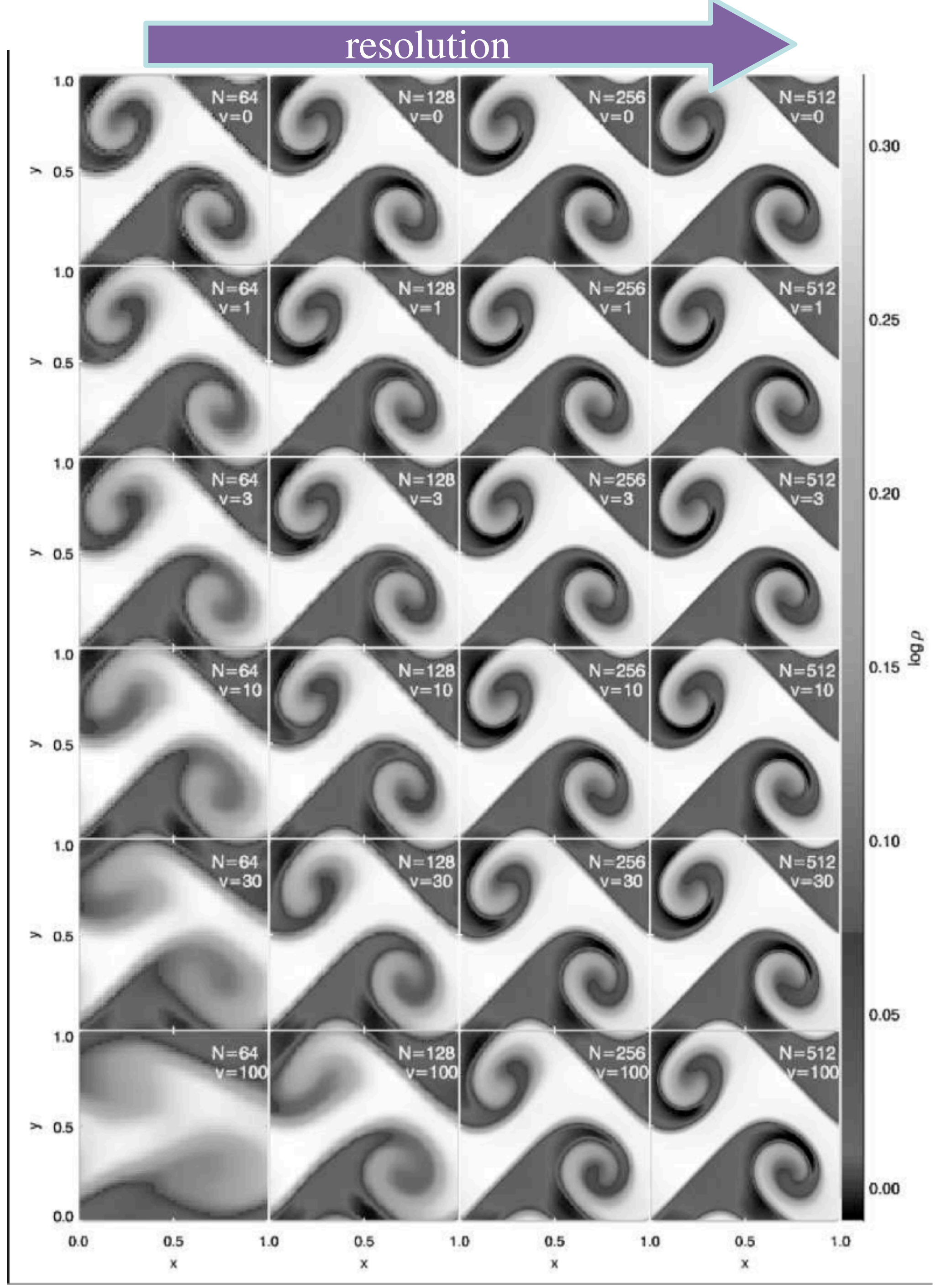

WHICH METHOD IS BEST?

Adaptive Mesh Refinement :

Eulerian method can increase the local spatial resolution where needed

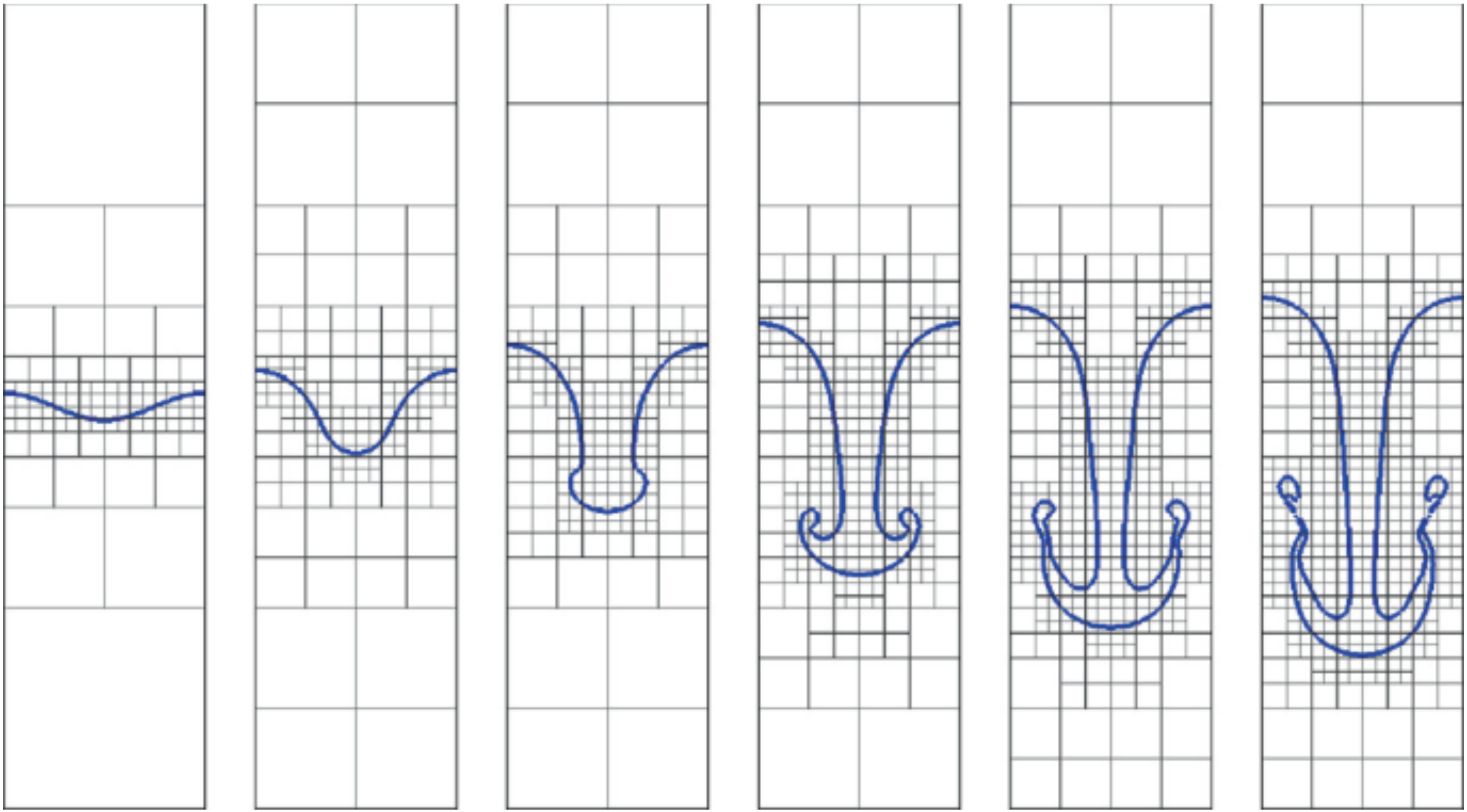

WHICH METHOD IS BEST?

Adaptive Mesh Refinement :

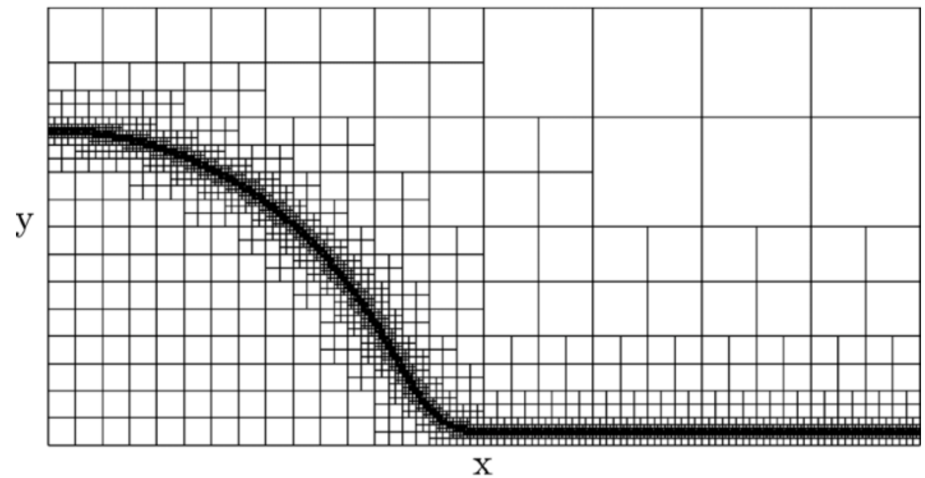

- in simulations of cosmic structures, finer grids are generated for example where the matter density increases because of gravitational collapse

- fluxes on coarse resolution levels are used as boundary conditions for high resolution cells

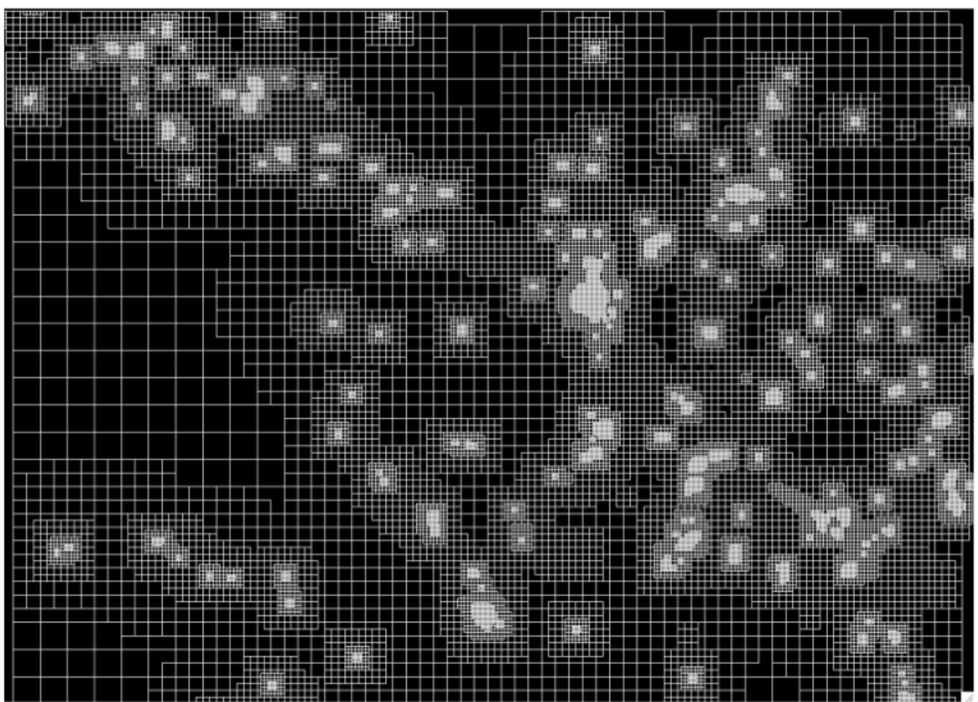

WHICH METHOD IS BEST? ADVECTION PROBLEMS

New methods to “combine the best of both worlds”:

- mesh continuously generated following moving mass points (→ galileian invariance, high resolution)
- fluid dynamics computed with Riemann solvers (→ accurate reconstruction of shocks, fluid instabilities)

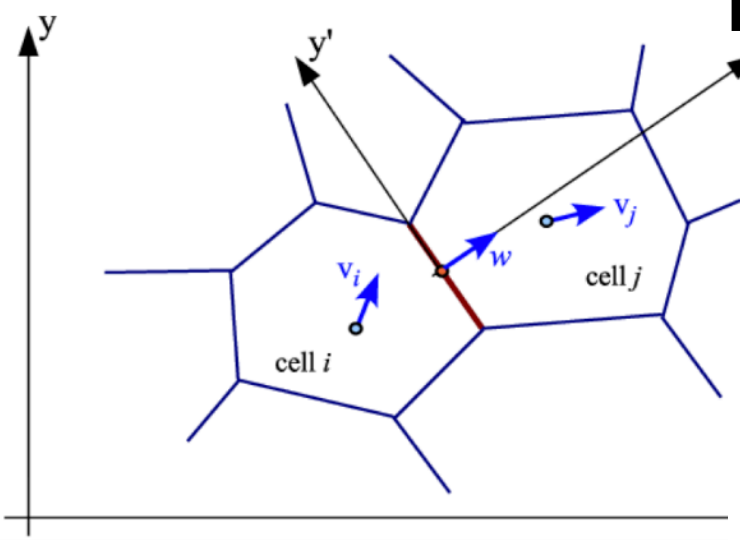

AREPO - Springel 2010

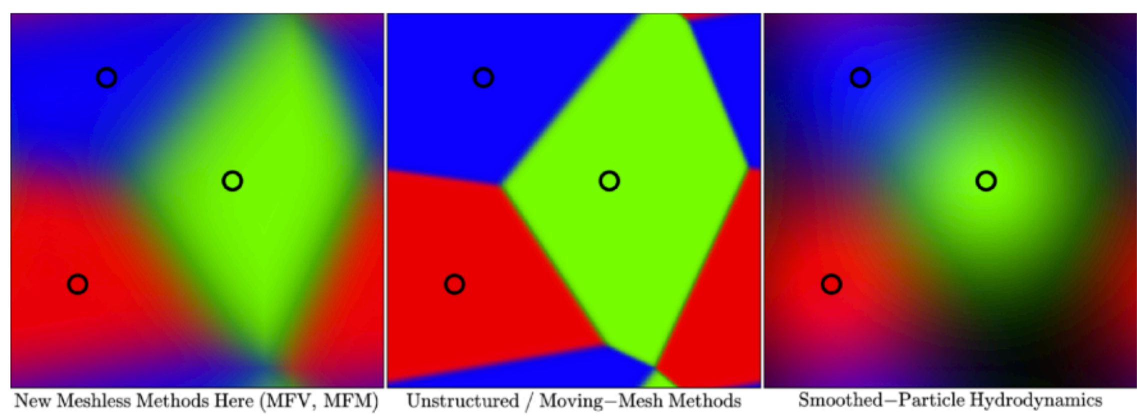

GIZMO - Hopkins 2015

WHICH METHOD IS BEST?   ADVECTION PROBLEMS

New methods to “combine the best of both worlds”:

- mesh continuously generated following moving mass points (→ galileian invariance, high resolution)
- fluid dynamics computed with Riemann solvers (→ accurate reconstruction of shocks, fluid instabilities)

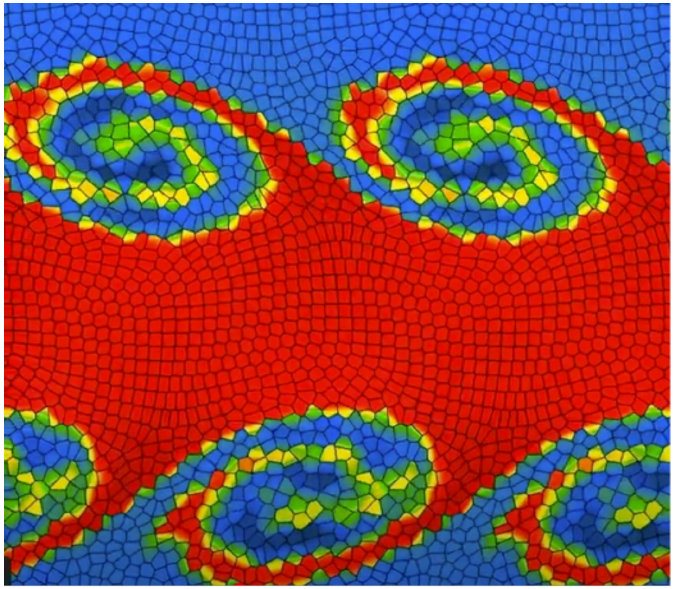

AREPO - Springel 2010

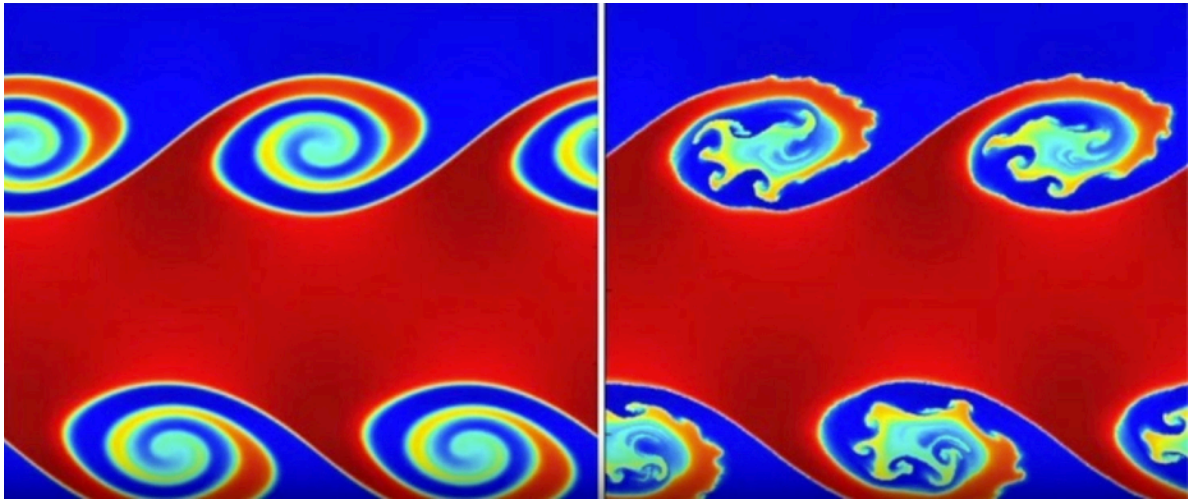

GIZMO - Hopkins 2015

Advantages/disadvantages of each method

Lagrangian: Moving volume element	Eulerian: Static volume element	Hybrid (moving-mesh)
Smears out shocks and discontinuities	Riemann solvers are great for capturing shocks!	Riemann solvers are great for capturing shocks!
Naturally Galilean-invariant	Truncation errors depend on velocities	Naturally Galilean-invariant

Choose a code according to the needs of your problem!

MORE COMPLICATIONS:

To form galaxies and their stars, much more is needed:

- cooling
- chemistry
- radiative transport
- star formation
- black holes
- feedback
- cosmic rays
- magnetic fields
- dust

etc…

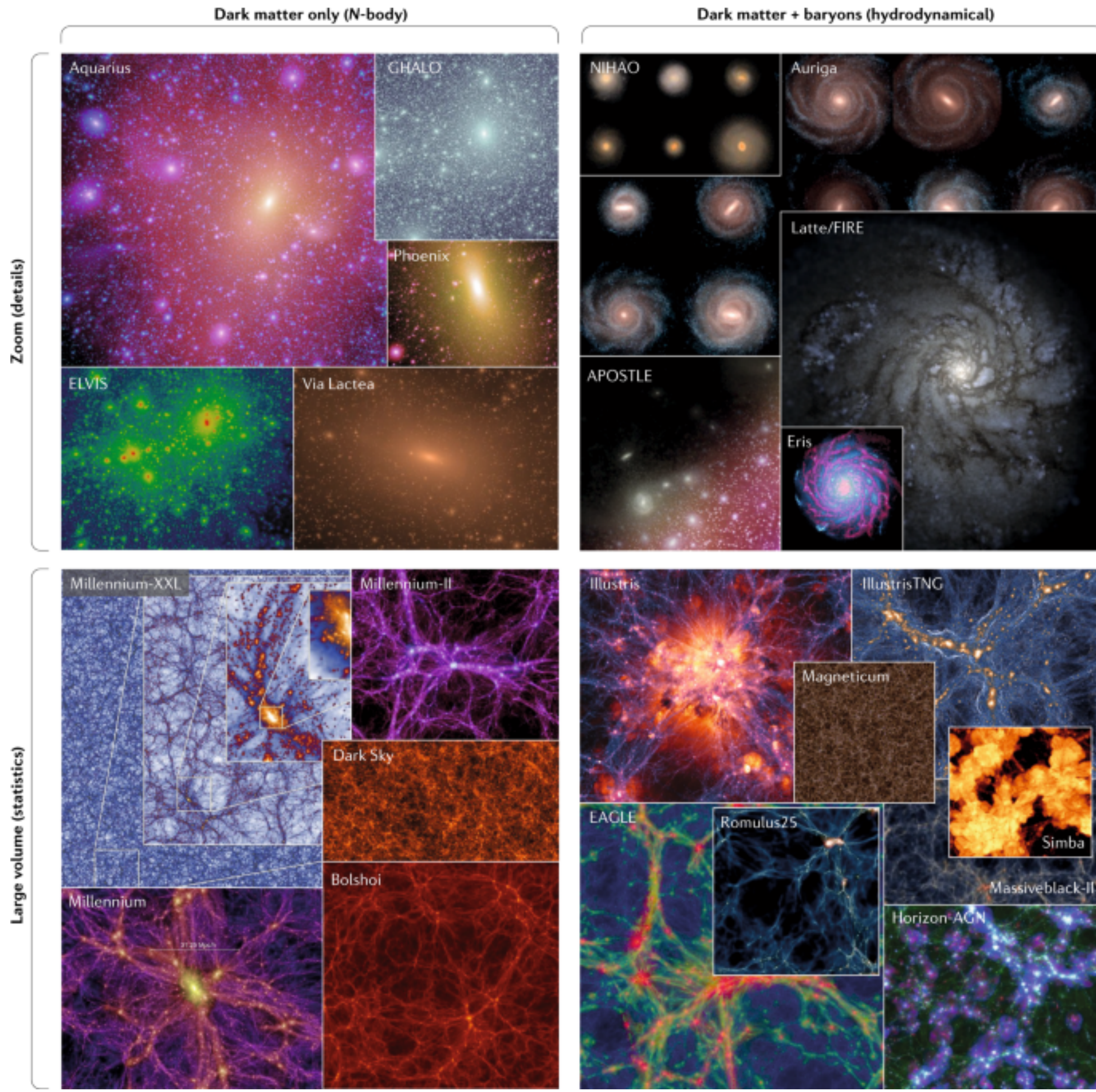

Vogelsberger+20

STAR FORMATION, FEEDBACK, ACTIVE GALACTIC NUCLEI

- turning gas into stars $\dot{\rho}_* = \epsilon_{\rm ff}\frac{\rho}{\tau_{\rm ff}}$ with $\tau_{\rm ff} = \sqrt{\frac{3\pi}{32G\rho}}$

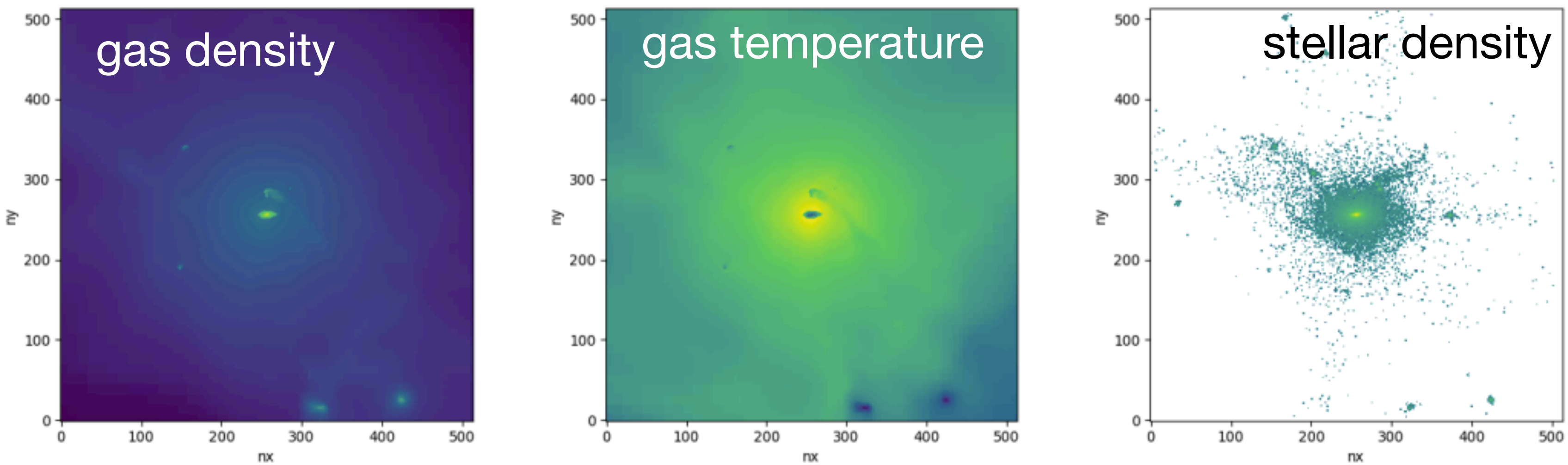

Figure 8: Left panel: projected density map of a zoom-in cosmological simulation of a Milky-Way-size halo with radiative cooling and no feedback. Middle panel: projected temperature map. Right panel: stellar surface density map. The image is 500 kpc across. Credit figure and simulation: R. Teyssier.

STAR FORMATION, FEEDBACK, ACTIVE GALACTIC NUCLEI

- turning gas into stars
- letting stars do feedback

$$\Delta m_{\rm host} = f_{\rm host} m_{\rm ej}$$

$$\Delta E_{\rm host} = f_{\rm host} E_{\rm SN} + \frac{1}{2} f_{\rm host} m_{\rm ej} \left| \mathbf{v}_* - \mathbf{v}_{\rm host} \right|^2 .$$

several possible implementations of feedback in numerics (thermal, kinetic, mechanical..); all are “true” at some given scale.

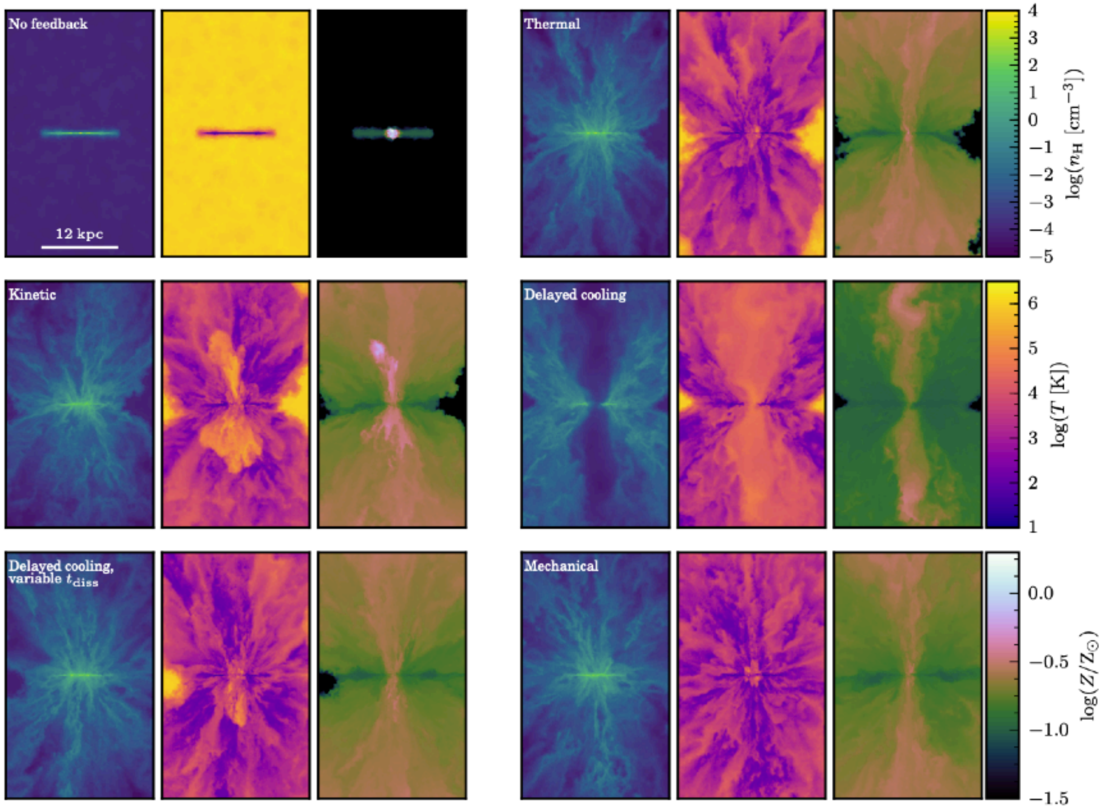

STAR FORMATION, FEEDBACK, ACTIVE GALACTIC NUCLEI

- turning gas into stars
- letting stars do feedback
- growing supermassive black holes

“seed” black holes (e.g. $M_{BH,seed} \sim 10^4 - 10^6 M_\odot$)
are injected in halos at high redshift

they grow matter based on either hot gas accretion
(Bondi-Hoyle formula)

$$\dot{M}_{\rm BH} = \min\left(\frac{4\pi\alpha G^2 M_{\rm BH}^2 \rho_{\rm B}}{c_s^3}; \frac{4\pi G M_{\rm BH} m_p}{\epsilon_r \sigma_T c}\right),$$

Bondi   Eddington limit

and/or cold gas accretion

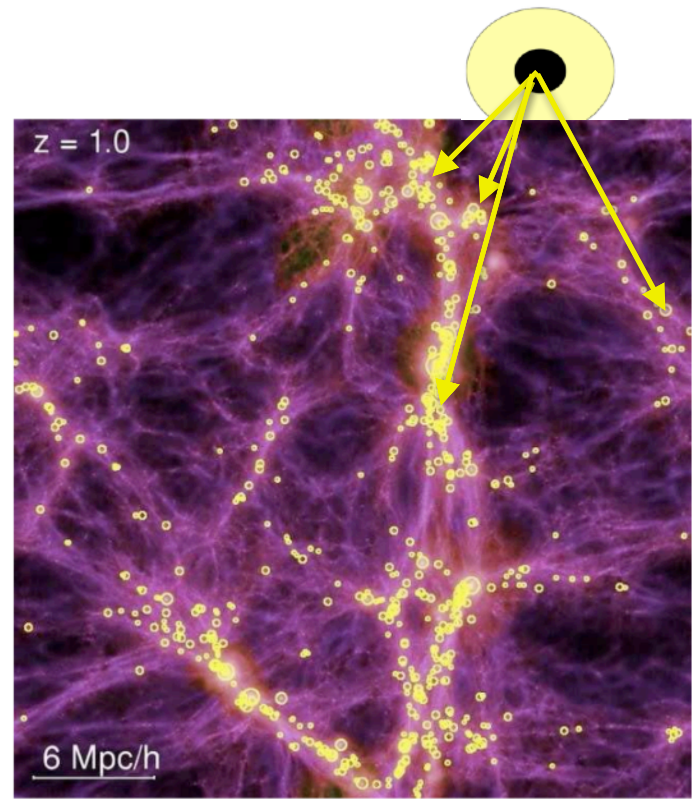

STAR FORMATION, FEEDBACK, ACTIVE GALACTIC NUCLEI

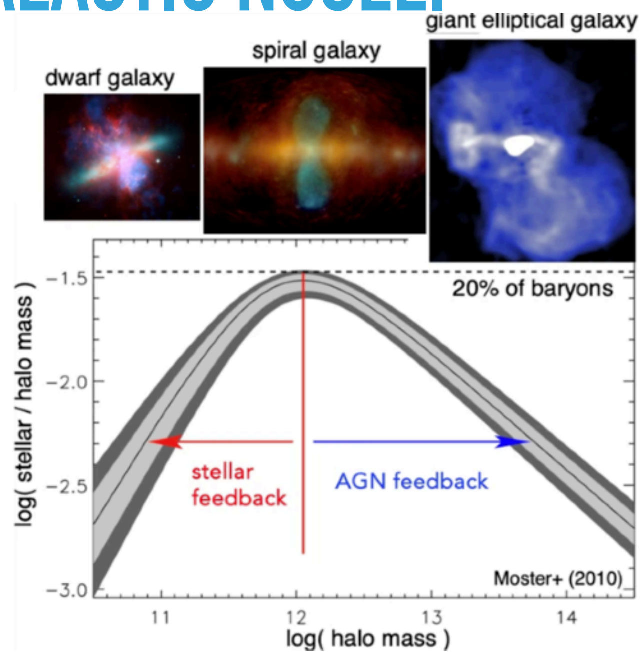

- turning gas into stars
- letting stars do feedback
- growing supermassive black holes
- letting supermassive black holes do feedback

A fraction ϵ_r of the accreted mass rate is released outwards as feedback energy $L_{BH} = \epsilon_r \dot{M}_{BH} c^2$

Numerical recipes have been implemented for radiative, mechanical, thermal feedback e.g. for mechanical feedback:

$$P_{\rm kin} = \epsilon_{\rm kin} L_{\rm BH} = \epsilon_{\rm kin}\epsilon_{\rm r} \dot{M}_{\rm BH} c^2 = \frac{1}{2}\dot{M}_{\rm jet} v_{\rm jet}^2,$$

$$v_{\rm jet} = c\left(\frac{2\epsilon_{\rm kin}\epsilon_{\rm r}}{\eta_{\rm jet}}\right)^{1/2} = 6000\ {\rm km\,s^{-1}}$$

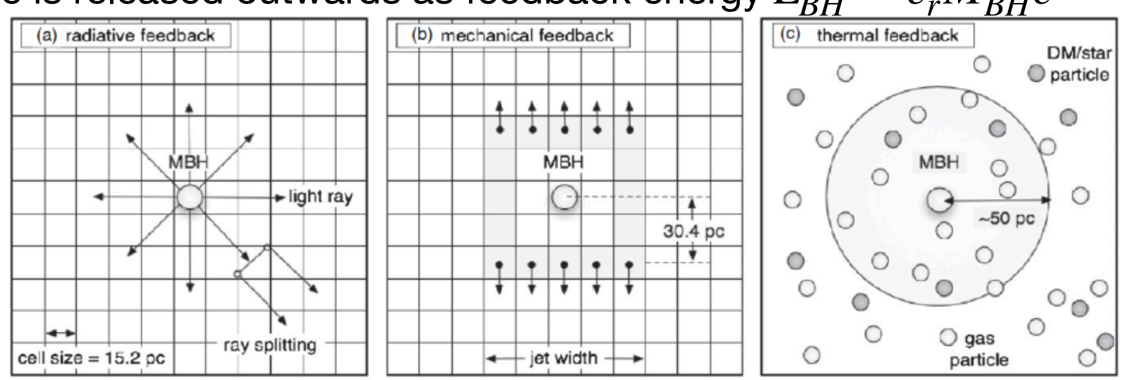

Figure 2. Two-dimensional schematic views of the different modes of massive black hole feedback. (a) Radiative feedback model described in Section 2.7: photon rays carrying the energy are adaptively traced via full radiative transfer, (b) mechanical feedback model described in Section 2.8: a momentum is injected to the cells around the MBH along pre-calculated directions, and (c) thermal feedback model predominantly used in particle-based galactic scale simulations: thermal energy is kernel-weighted to the neighboring gas particles around the MBH.

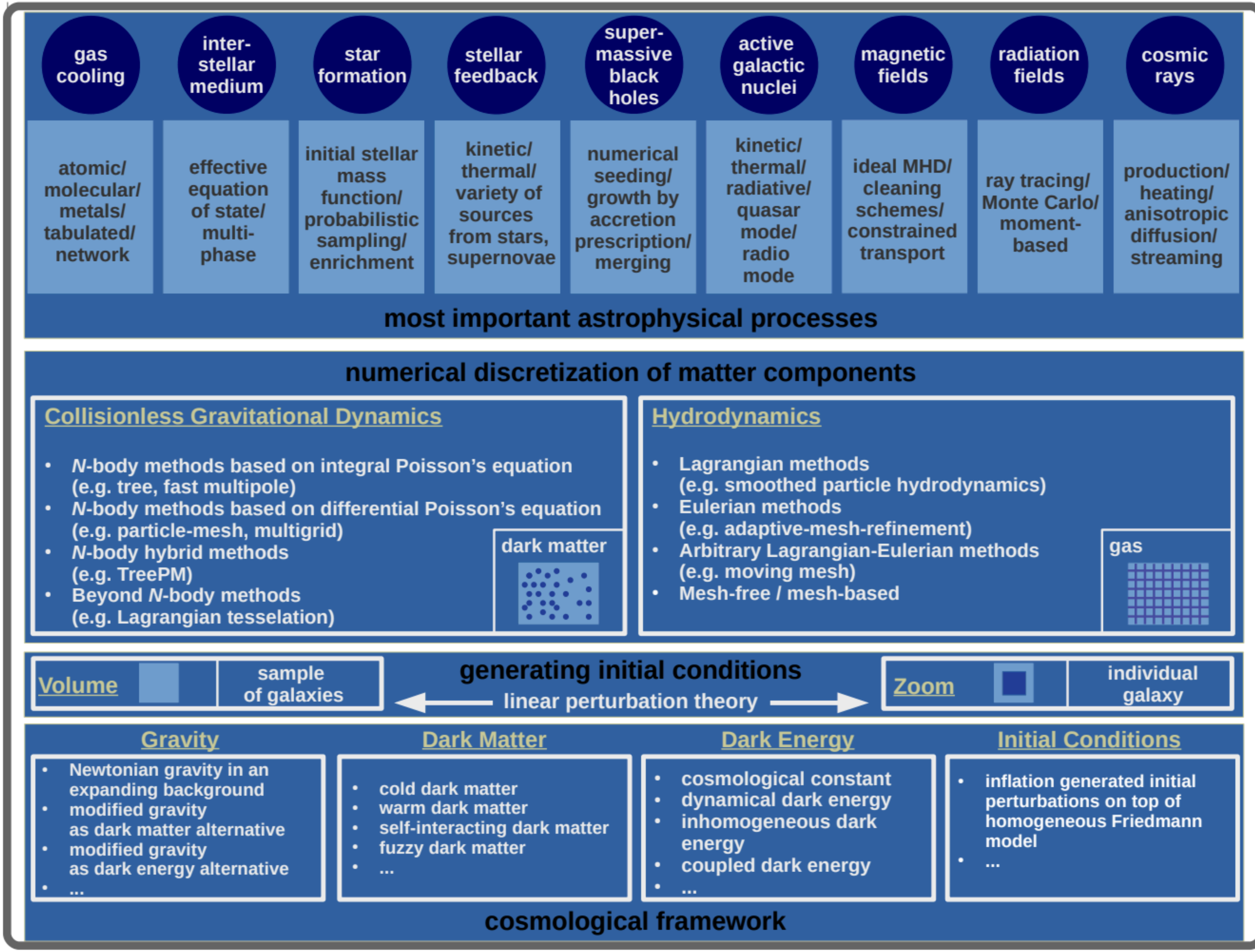

Vogelsberger+20

SIMULATING COSMIC RAYS IN COSMIC STRUCTURES

The usual equations must include a "two-fluid" model for cosmic ray protons

- continuity $$\partial_t \rho + \nabla \cdot (\rho \boldsymbol{u}) = 0,$$
- momentum conservation $$\rho\,(\partial_t \boldsymbol{u} + \boldsymbol{u} \cdot \nabla \boldsymbol{u}) = -\nabla(P_{\mathrm{TH}} + P_{\mathrm{CR}}),$$
- energy conservation $$\partial_t \epsilon_{\mathrm{TH}} + \nabla \cdot (\epsilon_{\mathrm{TH}} \boldsymbol{u}) = -P_{\mathrm{TH}}(\nabla \cdot \boldsymbol{u}) + \Gamma + \Lambda,$$
- CR energy conservation $$\partial_t \epsilon_{\mathrm{CR}} + \nabla \cdot (\epsilon_{\mathrm{CR}} \boldsymbol{u}) = -P_{\mathrm{CR}}(\nabla \cdot \boldsymbol{u}) + \nabla \cdot (\kappa_{\mathrm{CR}} \nabla \epsilon_{\mathrm{CR}}) + \Gamma_{\mathrm{CR}},$$
- state equations $$P_{\mathrm{TH}} = (\gamma_{\mathrm{TH}} - 1)\epsilon_{\mathrm{TH}},$$ $$P_{\mathrm{CR}} = (\gamma_{\mathrm{CR}} - 1)\epsilon_{\mathrm{CR}},$$
- source terms, diffusion of CRs…

SIMULATING COSMIC RAYS IN COSMIC STRUCTURES

Milky-way like galaxy:

Constant Diffusion

vs

Variable Diffusion

Semenov+21

→ more realistic diffusion make the CR distribution clumpier

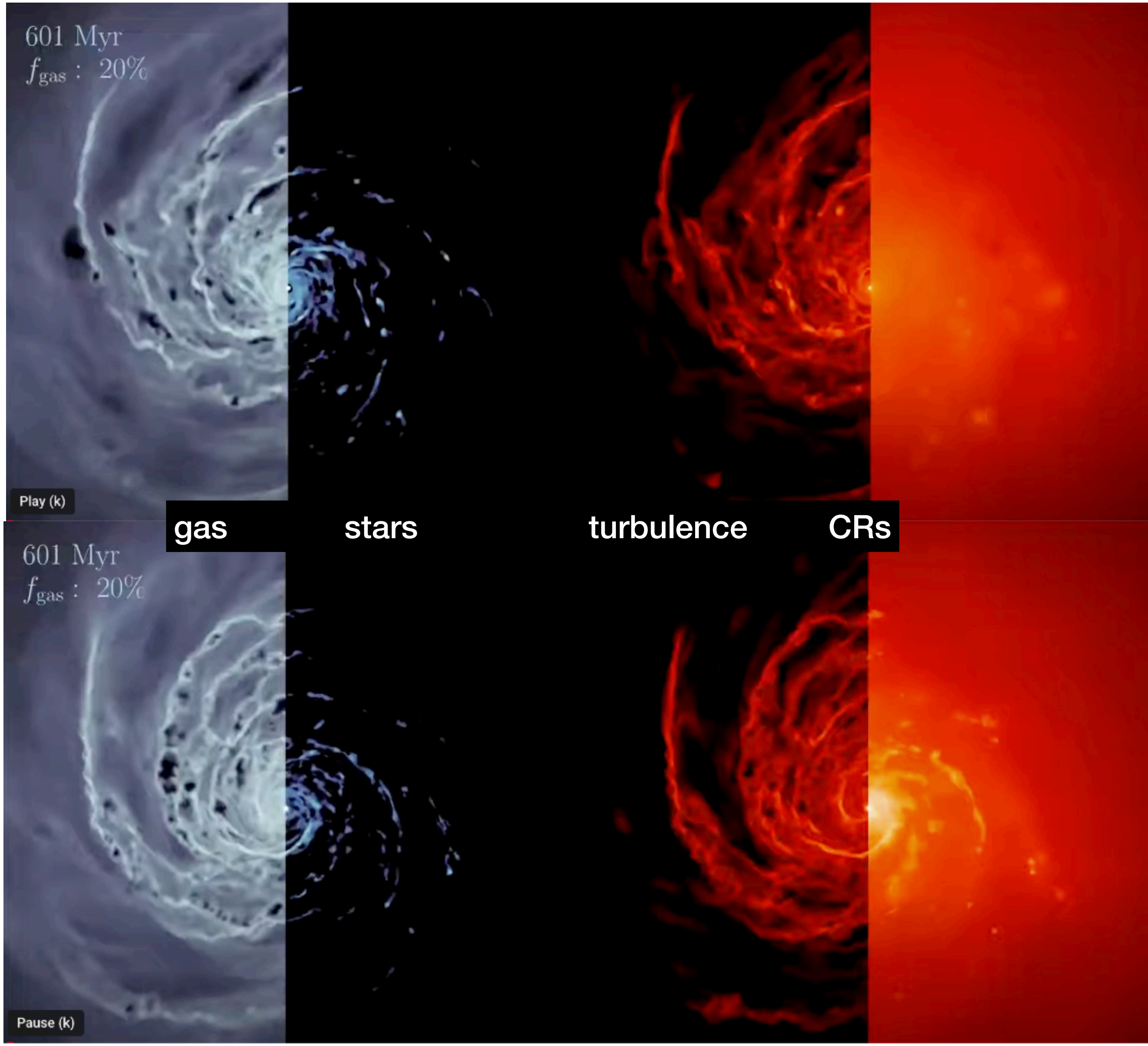

SIMULATING COSMIC RAYS IN COSMIC STRUCTURES

Once injected, the accelerated cosmic rays can be modelled as a second fluid which interact with the "normal" one of thermal gas, which evolves according to a $\Gamma = 4/3$ eq. of state.

The composite gas+CR fluid evolves according to an "effective" equation

of state:

$$\Gamma_{eff} = \frac{5/3E_g + 4/3E_{CR}}{E_g + E_{CR}} \leq 5/3$$

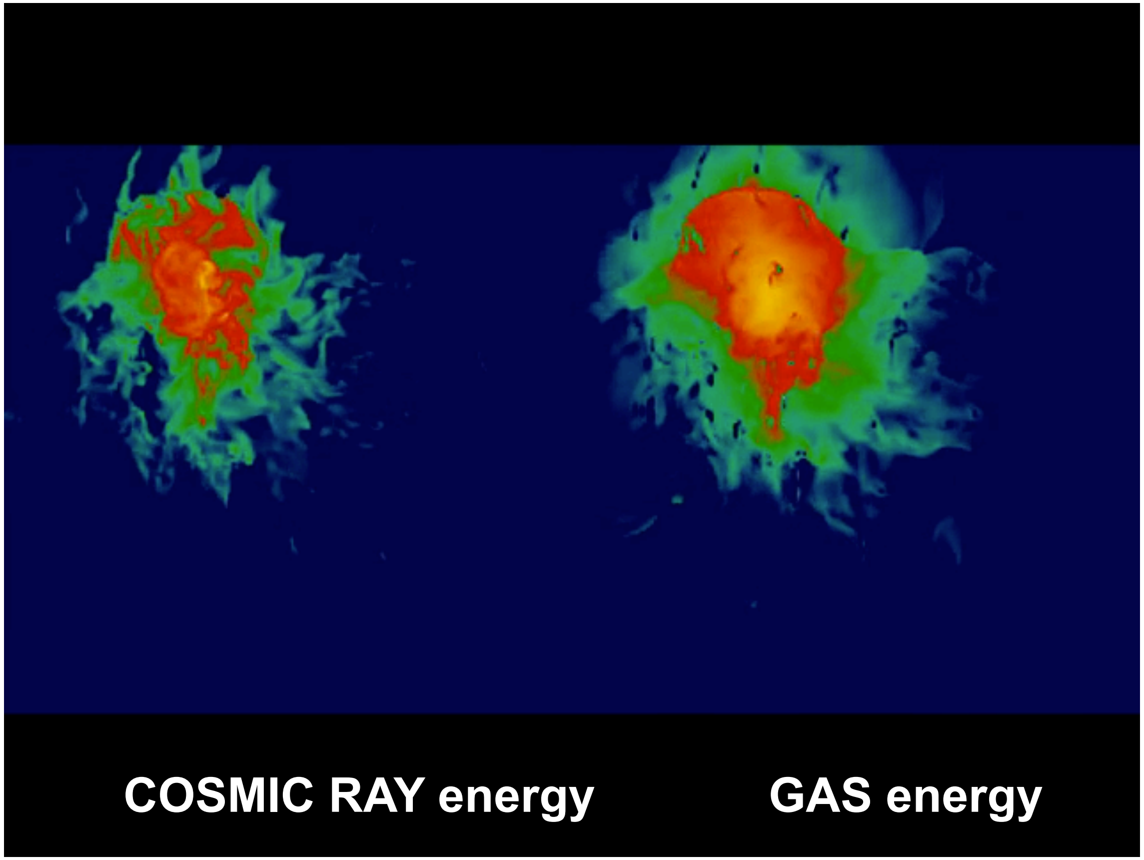

SIMULATING COSMIC RAYS IN COSMIC STRUCTURES

Simulated distribution of CRs (accelerated by cosmic shocks) in the cosmic web

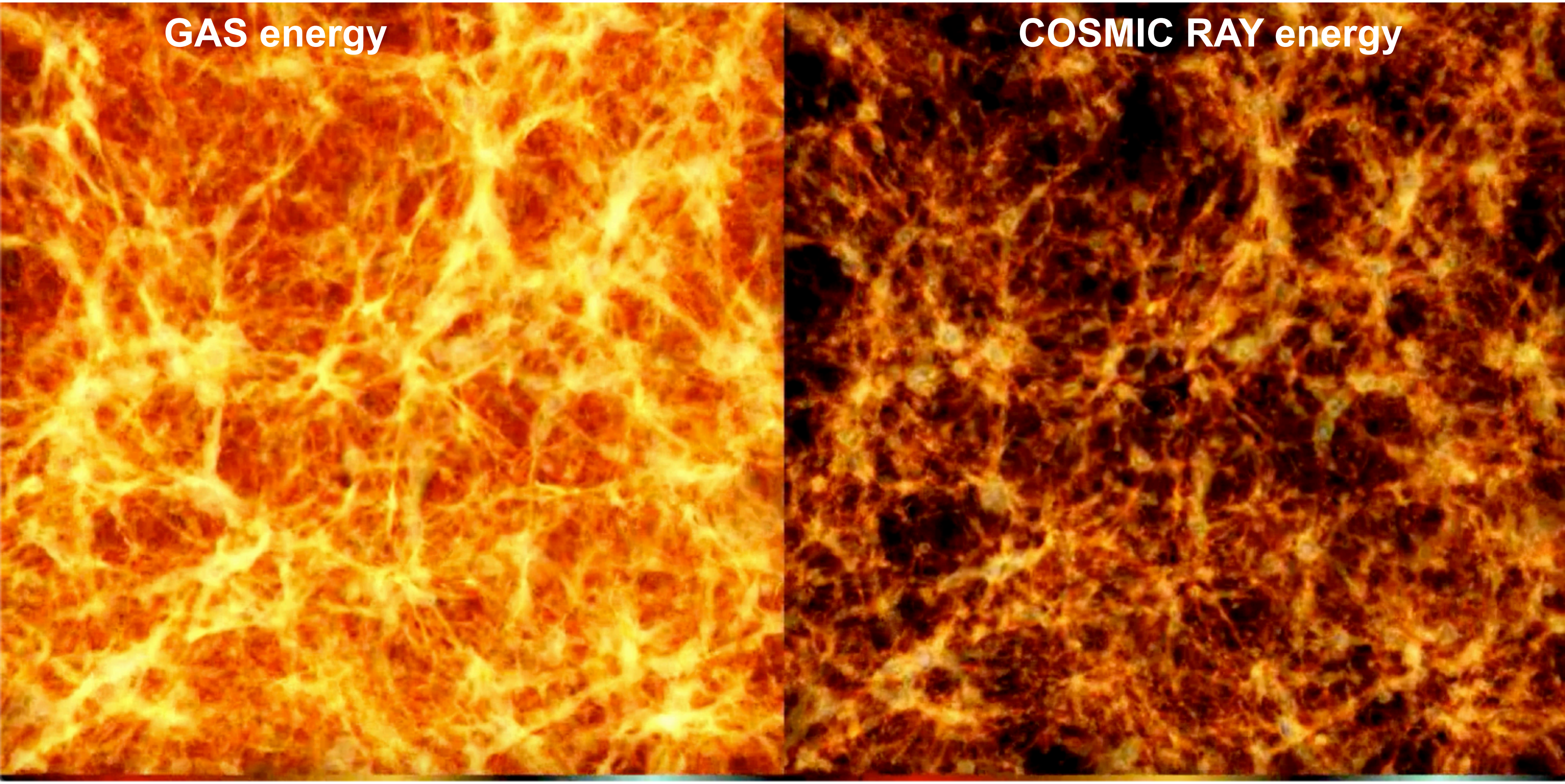

(Vazza+12)

SIMULATING COSMIC RAYS IN COSMIC STRUCTURES

Effect of cosmic ray acceleration in the density and temperature profile of a simulated galaxy clusters: a model with cosmic rays (**blue**) has a $\sim 5-10\,\%$ lower density and temperature than a standard model without cosmic ray effects (**black**). This is a combined effect of a reduced thermalisation at shocks ("thermal leakage") as well as of the $\Gamma_{\rm eff} \leq 5/3$ effective adiabatic index of gas.

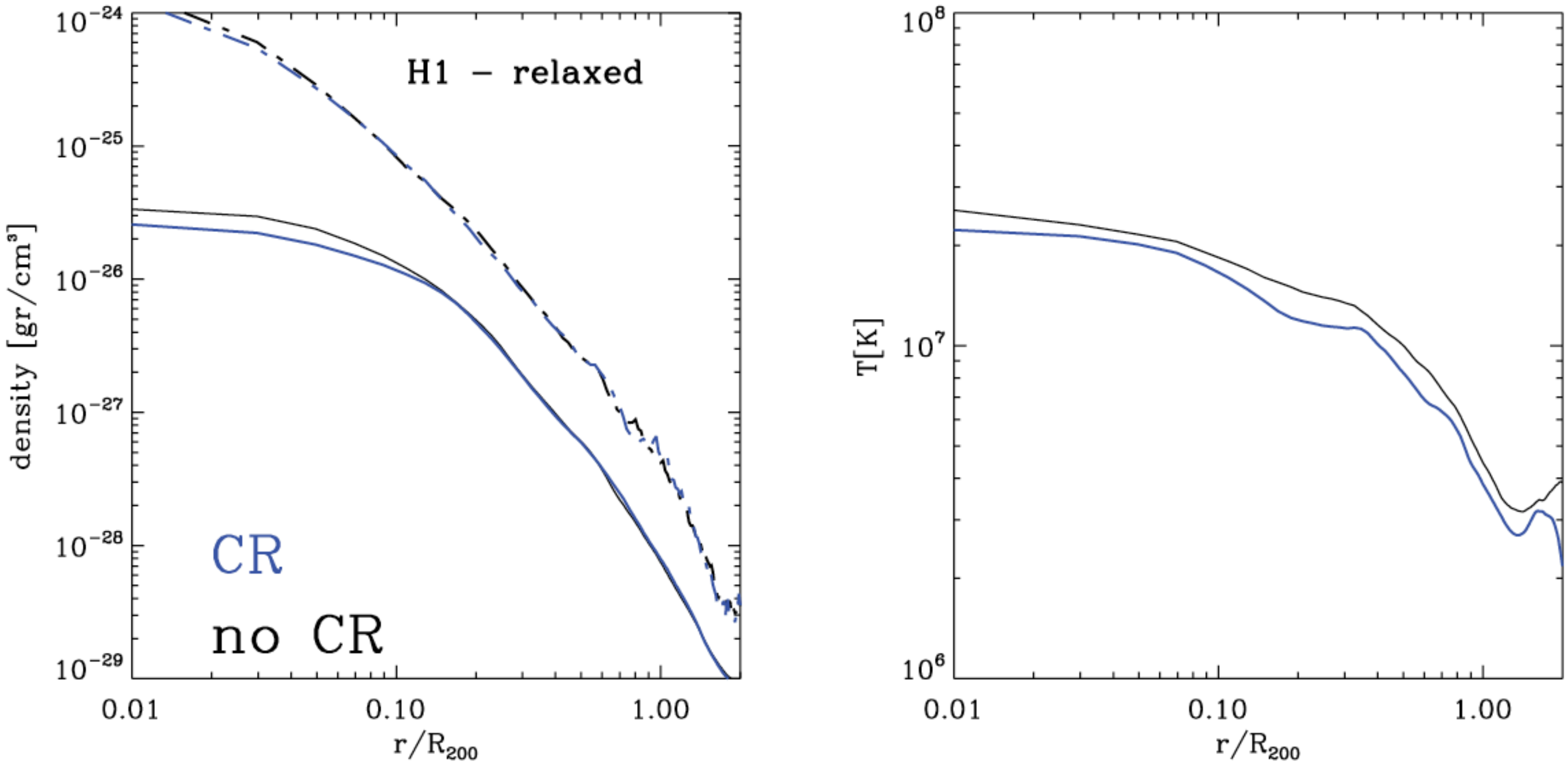

SIMULATING MAGNETIC FIELDS IN COSMIC STRUCTURES

New set of equations, now with links between gas and $\mathbf{B}$, for ideal MHD ((single fluid, no resistivity, large conduction)

- continuity

$$\frac{\partial \rho}{\partial t} + \frac{1}{a}\nabla \cdot (\rho \mathbf{v}) = 0, \quad (1)$$

- momentum conservation

$$\frac{\partial \rho \mathbf{v}}{\partial t} + \frac{1}{a}\nabla \cdot \left(\rho \mathbf{v}\mathbf{v} + \mathbf{I}p^* - \frac{\mathbf{B}\mathbf{B}}{a}\right) = -\frac{\dot{a}}{a}\rho \mathbf{v} - \frac{1}{a}\rho \nabla \phi, \quad (2)$$

- energy conservation

$$\frac{\partial E}{\partial t} + \frac{1}{a}\nabla \cdot \left[(E + p^*)\mathbf{v} - \frac{1}{a}\mathbf{B}(\mathbf{B}\cdot \mathbf{v})\right] = -\frac{\dot{a}}{a}\left(2E - \frac{B^2}{2a}\right) - \frac{\rho}{a}\mathbf{v}\cdot \nabla \phi - \Lambda + \Gamma + \frac{1}{a^2}\nabla \cdot \mathbf{F}_{\mathrm{cond}}, \quad (3)$$

- magnetic induction

$$\frac{\partial \mathbf{B}}{\partial t} - \frac{1}{a}\nabla \times (\mathbf{v} \times \mathbf{B}) = 0. \quad (4)$$

- $B = B_{proper}/a^2$

more on this on Thursday!

EFFECTS OF PMFS IN COSMOLOGICAL SIMULATIONS

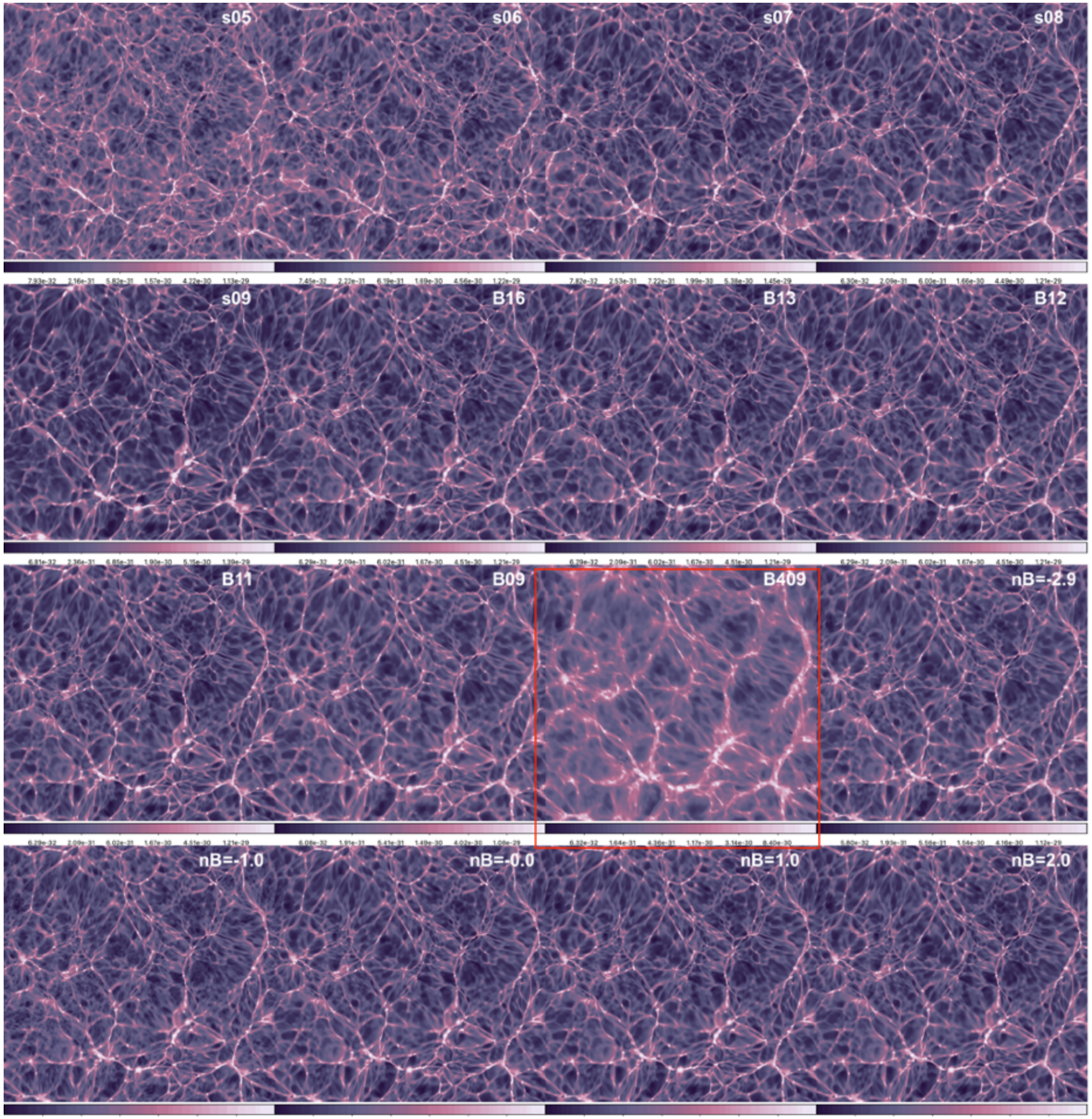

Simulated dynamical effects of PMFs on the growth of structures

Map: gas density distributions at z=0.2 for different simulations with varying normalisation and slope of PMFs, or of σ_8

[with 1 caveat:

B is here introduced only at the begin of the simulation ($z = 30$) but is not used to "perturb" the initial conditions obtained for ΛCDM…it is still diffcult!]

Rudakovskyi+25

EFFECTS OF PMFS IN COSMOLOGICAL SIMULATIONS

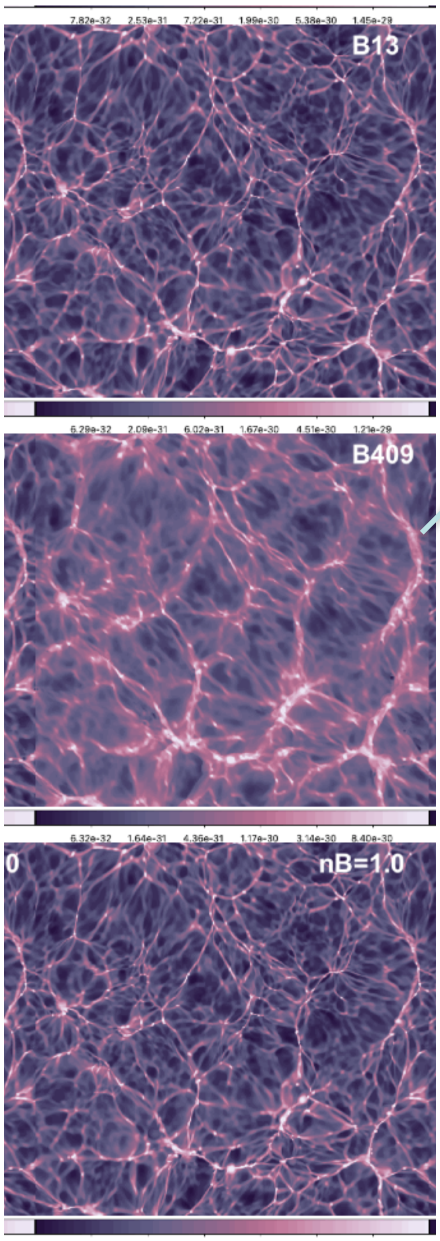

Simulated dynamical effects of PMFs on the growth of structures

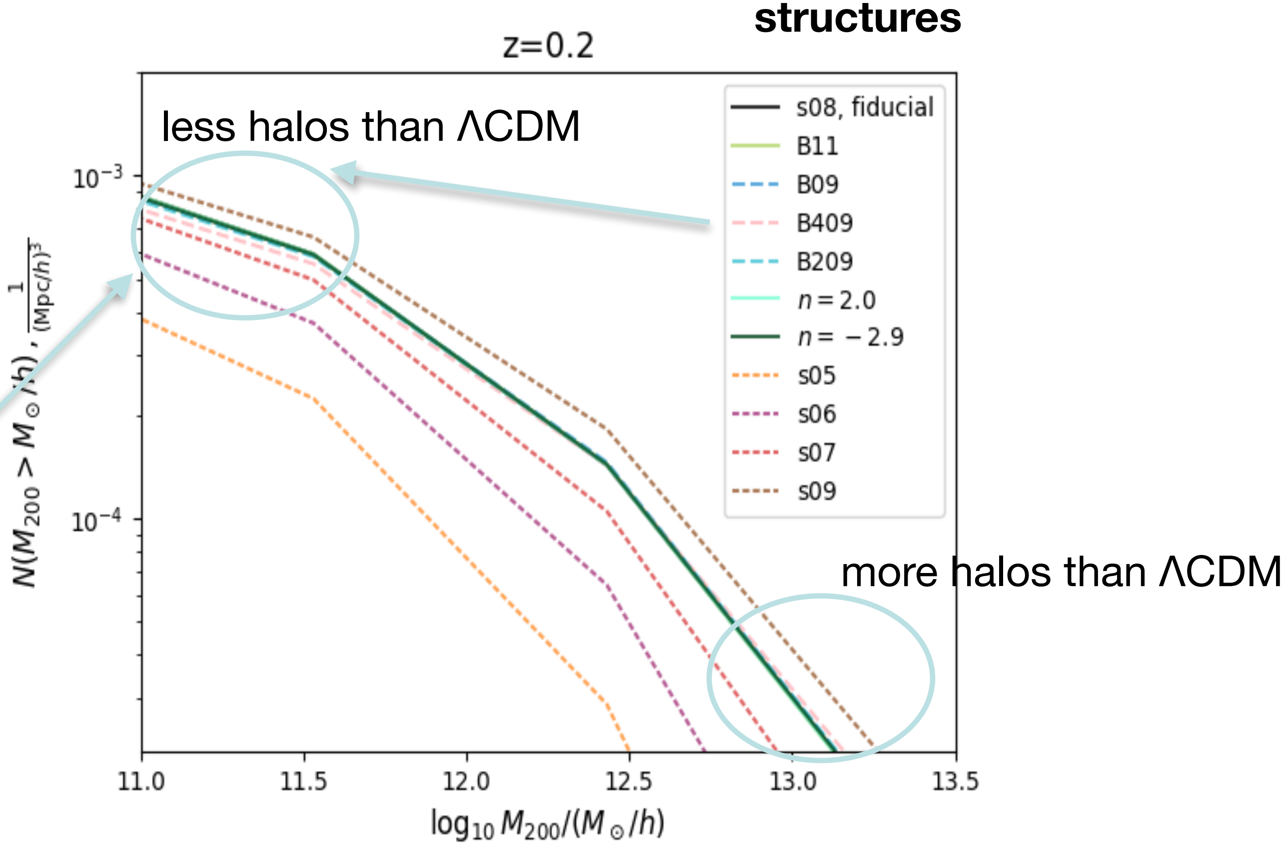

- B-fields $\geq 2\mathrm{nG}$ at $z = 30$ perturb the mass function similar to a slightly reduced σ_8 (i.e. $\sigma_8 \approx 0.75$) in ΛCDM
- Differences between scenarios are better highlighted by other diagnostics (e.g. network analysis)

Rudakovskyi+25

EFFECTS OF PMFS IN COSMOLOGICAL SIMULATIONS

Non linear modifications to the ΛCDM growth factor has started to be worked with full cosmological simulations (analytical T(k) transfer function for $n_B \leq -1.5$ spectra, with $P_B(k) \propto k^n$, or approximate solutions otherwise)

First cosmological MHD simulations with initial conditions perturbed by PMFs (here $n_B = -2$ and $B_{1Mpc} = 0.2\text{nG}$)

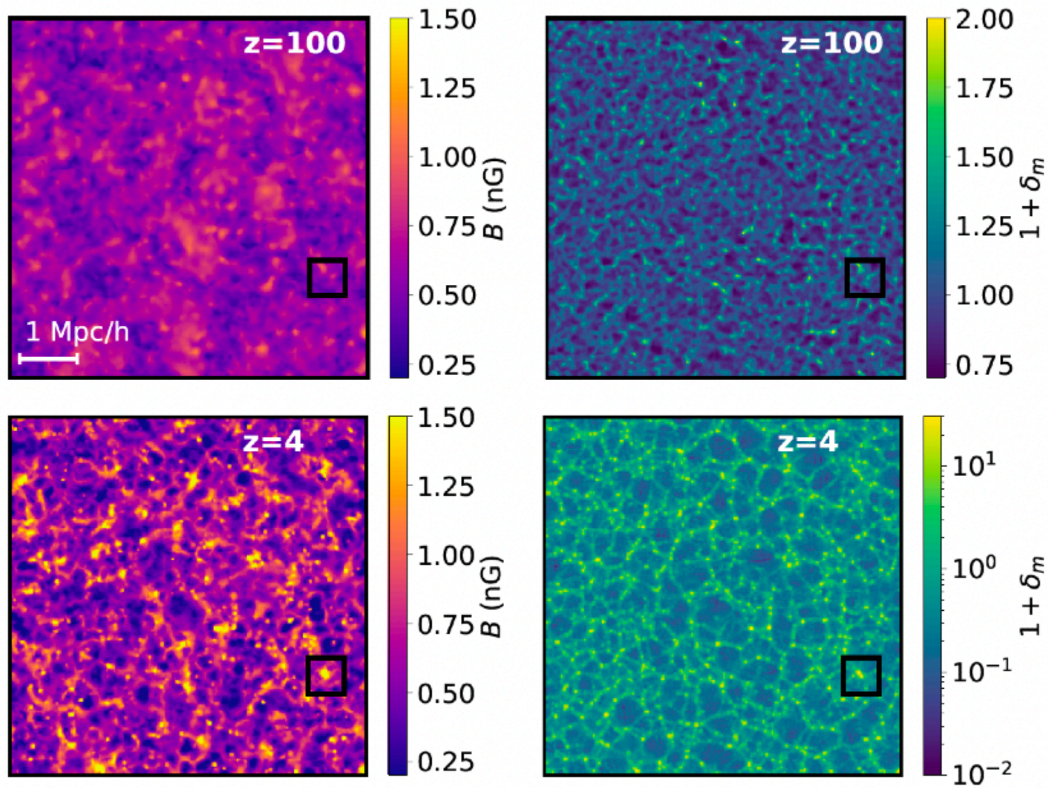

Figure 2. A thin slice of 0.3 Mpc/h is cut out of the simulation A volume and projected onto a 2D plane. This simulation has $B_{1\mathrm{Mpc}} = 0.2$ nG and $n_B = -2$. Left panel shows the map of PMF strength and the right panel shows the overdensity map of the total matter. The limits on the colour-bars are chosen manually for better visualization. These limits are not to be confused with the maximum/minimum values observed in the simulation. The square black box surrounds a region with an overdensity at $z = 4$.

EFFECTS OF PMFS IN COSMOLOGICAL SIMULATIONS

Non linear modifications to the ΛCDM growth factor has started to be worked with full cosmological simulations (analytical T(k) transfer function for $n_B \leq -1.5$ spectra, with $P_B(k) \propto k^n$, or approximate solutions otherwise)

- Magnetic-field dependent "boost" to the initial growth of $M \sim 10^5 - 10^{11}$ halos.
- On large scales, baryons can be initially more perturbed than DM

mass variance $\sim k^2 P(k)$ different simulated PMFs amplitudes/spectra:

compared to ΛCDM:

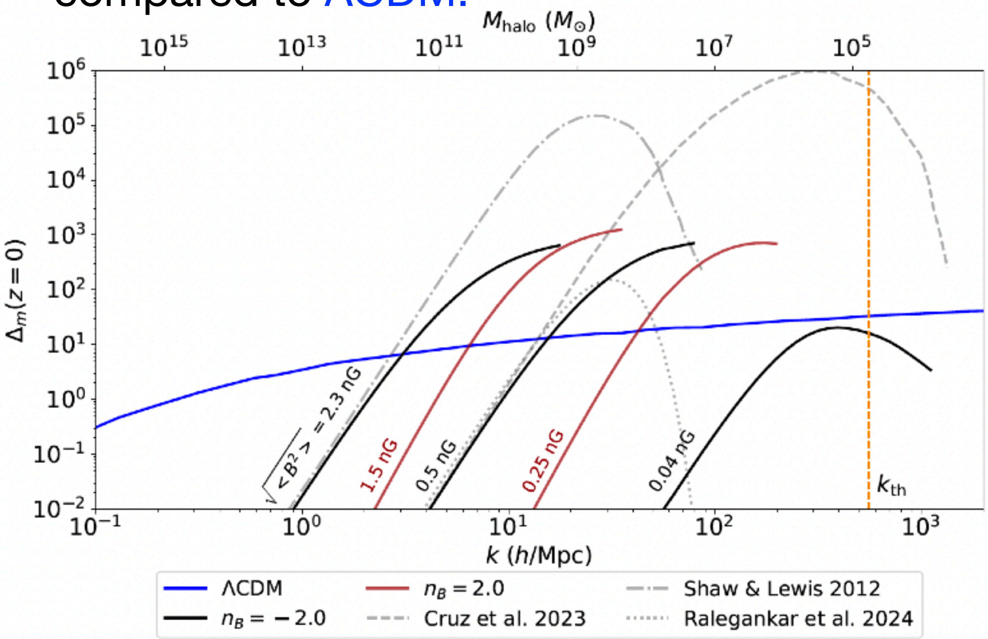

at different redshifts

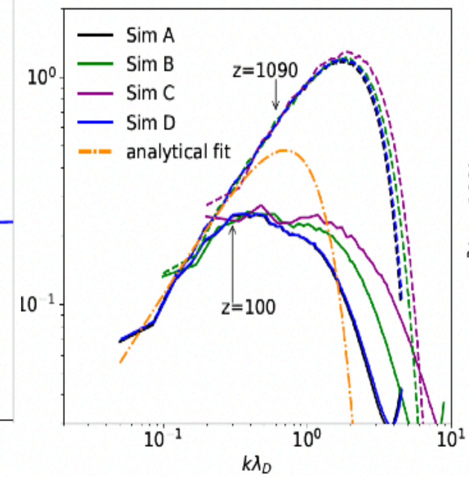

baryons vs DM

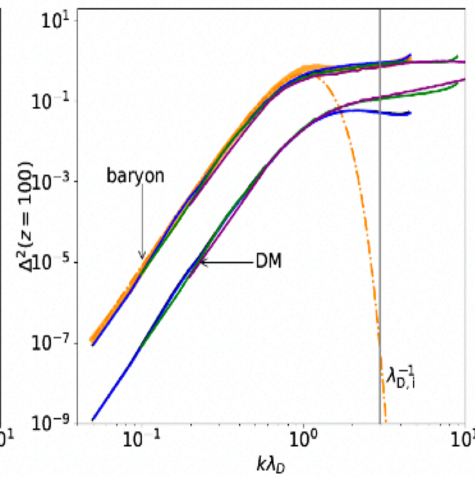

Ralengakar+25

EFFECTS OF PMFS IN COSMOLOGICAL SIMULATIONS

Cosmological simulations has started exploring in detail the different non-linear effects related to the possible presence of PMFs on different observable scales of the cosmic web

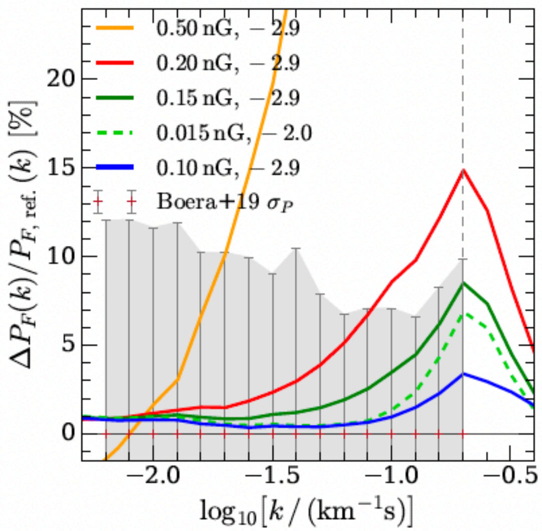

FIG. 2: Flux power spectra difference between PMF models at $z = 4.6$, where $\Delta P_F = P_F^{\mathrm{PMF}} - P_{F,\,\mathrm{ref.}}$, and the reference ΛCDM model. The shaded region with error bars show the observational 1σ uncertainty.

Modification of matter power-spectra, detectable via Lyman-α forrest:

Kahniashvili+2013, **Pavicevic et al 2025**

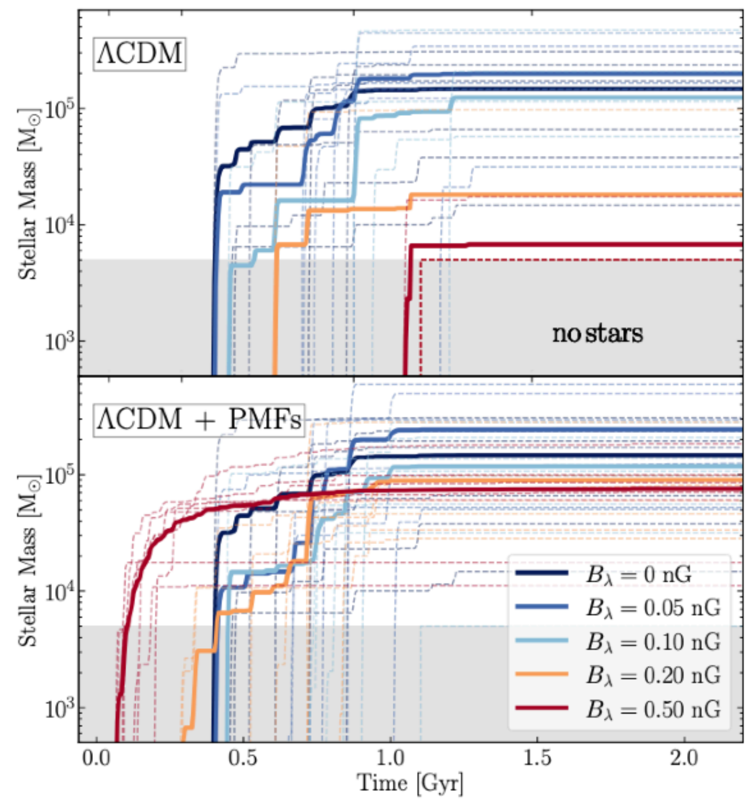

Change of the cosmic star formation history compared with ΛCDM

Sanati+2020,24 ; Ralegankar+24; Marinacci+15

EFFECTS OF PMFS IN COSMOLOGICAL SIMULATIONS

Working out the exact effect of magnetic fields on the growth of structures is not really trivial:

the force on baryons scales as

$$\mathbf{J} \times \mathbf{B} = \frac{(\mathbf{B} \cdot \nabla)\mathbf{B}}{\mu_0} - \nabla \left(\frac{B^2}{2\mu_0} \right)$$

and therefore it is also the topology of $\mathbf{B}$ which sets the force (not only the amplitude). Are PMFs clumpy or smooth? Tangled or regular?

e.g. very tangled PMFs with low normalisation can have more dynamical effects of smooth PMFs with higher normalisation.

…Full MHD simulations are necessary to work out $P_B(k)$ dependent effects

HAVE FUN:

A couple of online interactive tools to produce cosmological simulations:

https://www.galaxymakers.org/galform.php

https://galaxym.ovh/

SOME SUGGESTED READING

- *K. Dolag et al. 2008 "Simulation techniques for cosmological simulations"* *https://arxiv.org/pdf/0801.1023*
- *R. Teyssier 2025, "Numerical Cosmology"* *https://arxiv.org/pdf/2510.13129*